Studies on epigenetic mechanisms involved in the pathogenicity of Pyricularia oryzae

DANG NGOC MINH

(Degree)
博士（学術）

(Date of Degree)
2023-03-06

(Date of Publication)
2024-03-01

(Resource Type)
doctoral thesis

(Report Number)
乙第3428号

(URL)
https://hdl.handle.net/20.500.14094/0100482225

Doctoral Dissertation

Studies on epigenetic mechanisms involved in the pathogenicity of *Pyricularia oryzae*

(イネ科植物いもち病菌の病原性に関与するエピジェネティクス機構の研究)

DANG NGOC MINH

The Graduate School of Agricultural Science

KOBE UNIVERSITY

January, 2023

Contents

List of abbreviations

Abbreviations	Description
AGO	Argonaute
bp	Base pair
cDNA	Complementary DNA
CM	Complete medium
DCL	Dicer-like
DNA	Deoxyribonucleic acid
dsDNA	Double strand DNA
dsRNA	Double strand RNA
EDTA	Ethylendiamin tetraacetic acid
HYG	Hygromycin phosphotransferase cassette
KO	Knock out
LB	Luria-Bertani
LTR	Long terminal repeat
miRNA	Micro RNA
MSRE	Methylation sensitive restriction enzyme
nt	Nucleotide
OM	Osmotic medium
P. oryzae	*Pyricularia oryzae*
pBSKII	Plasmid Bluescript SKII
PCR	Polymerase chain reaction
PDA	Potato dextrose agar
PEG	Polyethylene glycol
qPCR	Quantitative polymerase chain reaction
qRT-PCR	Quantitative real time-polymerase chain reaction
RdRP	RNA-dependent RNA polymerase

RNA	Ribonucleic acid
RNAi	RNA interference
rRNA	Ribosomal RNA
siRNA	Small interference RNA
sRNA	Small RNA
sRNA-seq	Small RNA sequencing
ssRNA	Single strand RNA
STC	Sucrose Tris Calcium
TE	Transposable element
tiRNAs	tRNA-derived stress-induced RNAs
tRFs	tRNA-derived RNA fragments
tRNA	Transfer RNA
tsRNA	tRNA-derived small RNA

CHAPTER I

BACKGROUND INFORMATION

1. Epigenetics

Epigenetics refers to mechanisms that can induce heritable phenotypic changes without alterations in DNA sequence (Eccleston et al., 2007, Reik, 2007, Berger et al., 2009, Dupont et al., 2009). Specific epigenetic processes include post-transcriptional silencing, DNA modifications, maternal effects, X chromosome inactivation, histone modifications, transvection, the progress of carcinogenesis, as well as regulations by non-coding RNAs (Aristizabal et al., 2019) and so on. These mechanisms could activate or suppress gene expression, which leads to the proper differentiation of cells in multicellular organisms. Such impacts on the physiological characteristics of cells can be part of natural growth in response to external environmental factors.

2. Histone methylation

Histone methylation is a process in that methyl groups are added to lysine or arginine in histone proteins. Both histone arginine methyltransferases (RMTs) and lysine methyltransferases (KMTs) catalyze the transfer of methyl groups from S-adenosyl methionine to core histone proteins. Histone methylation is found on the amino termini of histones H1, H2A, H2B, H3, and H4. DNA genes are turned on and off by the methylation of the histones. Transcriptional factors and other proteins can access the target DNA region by losing the tails or encompassing the tails of histones (Jenuwein and Allis 2001). On histone arginine residues (R) usually occurs in mono- or di-methylated states while on histone lysine residues (K) are mono-, di- or tri-methylated. Methylated at histones H3 and H4 methylation gives the most biological influence (Jenuwein and Allis 2001). The number of methyl groups attached to histones greatly affects the transcription of DNA genes in that region (Zentner & Henikoff, 2013), for example, active transcription of the gene is usually associated with methylation of H3K4, H3K36, and H3K79

whereas the silencing is usually associated with methylation of H3K9, H3K27, and H4K20 (Black, Van Rechem, et al., 2012).

3. RNA interference

RNAi is an important epigenetic regulator in most eukaryotes. Initially, it describes post-transcriptional gene silencing by mRNA cleavage or translational inhibition. This phenomenon is known as co-suppression in plants, quelling in *Neurospora crassa,* and RNA interference in *C. elegans* and other animals (Lee et al., 1993; Napoli et al., 1990; Romano and Macino, 1992). Recently, it has been known that RNAi is involved in very dynamic crosstalk between transcription, histone modifications, and DNA methylation using small RNAs as a molecular guide for sequence specificity (Matzke et al., 2006; Slotkin and Martienssen, 2007; Moazed, 2009; Grewal, 2010).

Today RNAi is considered one of the new areas of research in the field of biology. Its importance has been evidenced by the 2006 Nobel Prize in Medicine for two American scientists, Dr. Andrew Z. Fire at Stanford University and Dr. Craig C.Mello at the Massachusetts University of Medicine. The molecular mechanism of gene silencing is divided into two stages based on genetic studies on *C. elegans* nematodes, plants, and biochemical research on Drosophila fruit flies (Bass, 2000). At the first stage, the dsRNA is decomposed by an enzyme belonging to RNase-III or DICER (Bernstein et al., 2001; Hammond et al., 2000; Kadotani et al., 2004) into shorter sections with a length of about 21-25 nucleotide sequences called small interfering RNA (Elbashir et al., 2001; Zamore et al., 2000). In the later stage, siRNA is incorporated into the protein complex called RISC (Hammond, 2000). Activated RISC uses single-stranded siRNA molecules to direct target messenger RNA molecules for degradation (Hammond, 2001).

RNA silencing components such as Dicer, RdRP, and AGO are widely conserved in plants, animals, fungi, and protists (Cerutti and Casas-Mollano,

2006; Chen, 2009; Kim et al., 2009; Castel and Martienssen, 2013). In the genome of the fungus *P. oryzae*, three RdRPs, MoRdRP1 (MGG_13453), MoRdRP2 (MGG_02748), MoRdRP3 (MGG_06205); two Dicer-like, MoDCL1 (MGG_01541), MoDCL2 (MGG_12357); and three Argonautes, MoAGO1 (MGG_01294), MoAGO2 (MGG_14873), MoAGO3 (MGG_13617) were identified. In *P. oryzae*, siRNAs sized from 19 to 23 nt were detected during gene silencing induced by hairpin RNA-producing constructs (Kadotani et al., 2003). This silencing was supposed to be due to post-transcriptional RNA degradation since no DNA methylation on the promoter and coding sequences were detected (Kadotani et al., 2003).

4. RNAi components

4.1. DCL

Dicer is a ribonuclease III-like enzyme that plays a crucial function in th e RNA silencing pathway. The genome sequencing programs have shown that eukaryotic genomes range from one (human) to four (Arabidopsis) in the number of DCLproteins. The smallest and shortest RNase III proteins are present in bacteria, bacteriophages with a single domain of ribonuclease (RIII) and a dsRBD.

Being a part of the RNase III family, Dicer cleaves dsRNA and pre-microRNA (pre-miRNA) into short dsRNA fragments referred to as siRNA and miRNA, respectively. These fragments are about 19-25 base pairs in length with a two-base overhang at the 3' ends. Dicer allows the activation of RISC that contains a catalytic factor Argonaute, an endonuclease able to degrade target mRNA.

4.2. RdRP

An enzyme catalyzing RNA replication from an RNA substrate is the RNA-dependent polymerase RNA or RNA replicase. The RNA transcription

process is a two-stage cycle. First, the initiation stage of RNA synthesis starts at or near the 3' end of the RNA template, using either a primer-independent (de novo) or a primer-dependent mechanism that uses RNA-binding protein such as viral protein genome-linked. De novo activation involves adding a triphosphate nucleoside to the 3'-OH of the first initiating NTP. The transition of nucleotidyl is repeated with subsequent NTPs during the following elongation stage to generate the complementary RNA strand (Kao et al., 2001). In the early 1960s, viral RdRPs were discovered from experiments on the mengovirus and poliovirus, where it was found that these viruses were insensitive to actinomycin D, a drug that inhibits RNA synthesis guided by cellular DNA. This lack of sensitivity indicated there is a virus-specific enzyme that may replicate RNA from an RNA template. In 2003, Iyer reported that several eukaryotes do have RdRPs functioning in the RNA interference pathway in which double-stranded RNA works as a trigger to induce the pathway and as a substrate for siRNA biogenesis. In early studies on transgene associated RNA silencing, it was proposed that cellular RdRP generates dsRNA using target mRNAs as a template, which is further processed into siRNA to provide the sequence specificity of the silencing (Lindbo et al, 1993). The unexpected potency, distribution, and durability of RNA silencing indicated potential amplification of the triggering RNA signals by RdRP. RNA silencing can be caused by injecting a small number of dsRNA molecules per cell but it spreads systemically to other parts of the body in animals and plants and persists in untreated progeny from treated parents (Bernstein et al., 2001).

4.3. Ago

The protein family Argonaute is a group of proteins that play key roles in RNA interference and its associated pathways. The existence of conserved domains such as PAZ, MID, and PIWI distinguishes its members (Tolia and

Joshua-Tor, 2007). In downstream gene silencing activities such as mRNA degradation, translational inhibition, and/or heterochromatinization, an AGO protein usually forms a protein complex containing sRNA as a specificity determinant (Moazed, 2009; Siomi et al., 2011).

AGO proteins in the three domains of life are evolutionarily conserved. For instance, there are 27 in *Caenorhabditis elegans*, while there is 1 AGO gene in *Schizosaccharomyces pombe,* and are 8 in *Homo sapiens* (Hock and Meister, 2008), indicating that pathways for the regulation of AGO-mediated genes may be diverse among species. Numerous AGO proteins in an organism with certain degrees of similarity between members often have distinct functions in the protection of growth and/or genomes. Both AGO4 and AGO6 are involved in the RNA-directed DNA-methylation pathway in Arabidopsis. Recent experiments, however, have shown that AGO4 and AGO6 are spatially distributed differently within the nucleus, and have distinct but cooperative roles in RdDM. AGO1 and AGO10 participate in the binding of target miRNA (Mallory et al., 2009). The competitive binding for miR166/165 between AGO1 and AGO10 is important for regulating shoot apical meristem development (Zhu et al., 2011). Therefore, the relationship among AGO proteins may be independent, mutual, or competitive.

5. *Pyricularia oryzae*

Rice is one of the five most important food crops in addition to wheat, corn, cassava, and potatoes. Rice is a very ancient crop in Asia, Africa, and Latin America. Currently, rice is the main food that feeds about 3.5 billion people, accounting for 50% of the world's population. According to FAO, in 2015, world rice production reached 749.1 million tons, of which Asian countries produced 677.7 million tons, accounting for 90.5% of the world's production. Due to the trend of expanding the area and intensive farming for a long time, pests on rice are widespread and difficult to control. One of the

most dangerous pests on rice is blast disease caused by *Pyricularia oryzae* (synonym: *Magnaporthe oryzae*). Blast disease causes an average yield loss of 0.7 to 17.5% but severe disease damage can be up to 80% (Bonman et al., 1986). This means rice blast can cause food shortage for several hundred million to several billion people a year. This disease is reported to occur in more than 80 rice-growing countries around the world. Elucidation of the pathogenesis of the rice blast fungus is crucial to the development of a new management method.

The infection cycle of *P. oryzae* consists of several steps. Vegetative hypha is easily grown in the laboratory and can be used to produce three-celled asexual spores, called conidia. Conidia are the principal source of inoculum in the field. A sequence of developmental events takes place after the landing of conidia on the surface of host leaves. These activities include germination of conidia, germ tube formation, and appressorium formation. A penetration peg arises from mature appressoria, which penetrates physically into host cells (Galhano and Talbot, 2011). After penetration, primary hyphae in the host cell can be classified into bulbous invasive hyphae and extra-invasive hyphal membranes.

CHAPTER II

MOSET1-DEPENDENT TRANSCRIPTION FACTORS REGULATE DIFFERENT STAGES OF INFECTION-RELATED MORPHOGENESIS IN *PYRICULARIA ORYZAE*

1. Introduction

The blast fungus, *P. oryzae* shows drastic morphological changes during the infection cycle (Talbot, 2003). Following attachment on the host leaf surface, a spore germinates and forms an appressorium at the tip of the germ tube. At the base of the appressorium, a penetration pore and peg are formed to colonize a host cell with infection hyphae. These morphological changes are accompanied with remarkable changes in gene expression (Jeon et al., 2020) that may involve cell type-specific epigenetic control of chromatin structure.

In *P. oryzae*, gene deletion analysis of eight possible KMTs revealed that MoSET1 responsible for H3K4 methylation plays a pivotal role in infection-related morphogenesis of the fungus (Pham et al., 2015a). Loss of MoSET1 led to a deficiency in cell growth, sporulation, appressorium formation, production of cell wall degradation enzymes, and pathogenicity (Vu et al., 2013; Pham et al., 2015a, b). RNA-seq analysis suggested that approximately 2,000 genes were up- or down-regulated during appressorium formation in a MoSET1-dependent manner. However, ChIP-seq analysis of MoSET1 protein revealed that only approximately 400 of the MoSET1-dependent genes were directly regulated by MoSET1 (Pham et al., 2015a), suggesting the involvement of a signaling cascade starting from MoSET1. In fact, the 400 genes contained possible signal mediators such as transcription factors and kinases.

In this chapter, I focus on MoSET1-dependent TFs. In fungi, TFs are key players in the signal transduction pathways and regulatory mechanisms (Shelest, 2008). For instance, Gomi and his coworkers (2000) stated that the deletion of AmyR, a zinc binuclear cluster DNA-binding protein in the Gal4p TF family, led to a decrease in amylolytic enzyme activities and vegetative growth of *Aspergillus oryzae* on starch medium. In *Parastagonospora*

nodorum, PnPf2, a TF belonging to the Zn2-Cys6 zinc finger subfamily positively regulated necrotrophic effector proteins and played an important role in the virulence on wheat (Jones et al., 2019). In *P. oryzae*, systematic analyses of the Zn2-Cys6 TF family and the Cys2-His2 zinc finger TF family were conducted (Lu et al., 2014; Cao et al., 2016) to reveal that 61 of 104 Zn2-Cys6 TFs and 44 of 47 Cys2-His2 TFs were involved fungal development and infection-related morphogenesis such as growth, conidiation, appressorium formation and pathogenicity (Lu et al., 2014; Cao et al., 2016). Among the 22 Cys2-His2 TFs required for the full virulence of the fungus, 2 were MoSET1-dependent TFs.

Here the functional analysis of five MoSET1-dependent TFs was carried out to explore their roles in the pathogenicity of *P. oryzae*. The results suggested that MoSET1 orchestrates various TFs to achieve successful infection of host plants with *P. oryzae.*

2. Materials and methods

2.1. Fungal strains and host plants

The wheat-infecting *P. oryzae* strain Br48 was collected in Brazil (Urashima et al., 1999). Fungal strains were preserved on barley seed media at 4^{o}C for long-term storage, and cultured on potato dextrose agar at 25^{o}C for working stock. “Norin 4” (N4), a cultivar of common wheat (*Triticum aestivum* L.) was used as a host plant of the Br48 strain.

2.2. Construction of gene knock-out and -down mutants

The split-maker disruption method (Catlett et al., 2003) was applied to construct deletion mutant strains (Fig. 2-1). First, up- and down-stream flanking regions of a target gene were amplified by PCR using KOD-Plus-Neo polymerase (TOYOBO, Osaka, Japan) and individually cloned by blunt-end ligation at *Pvu*II and *Eco*RV sites of pSP72-hph

containing a hygromycin B phosphotransferase gene (Hph) (Morita et al., 2013). Using the resulting plasmids, two DNA fragments containing a part of Hph and the flanking genomic region were amplified by PCR using KOD-Plus-Neo polymerase as shown in Fig. 2-1. The PCR products were purified using Wizard SV Gel and PCR Clean-up System (Promega, Madison, USA) after agarose gel electrophoresis, and used for fungal transformation. A list of primers used to amplify the genomic fragments was given in Table 2-1.

A retrotransposon-based gene silencing vector, pSilent-MG (Vu et al., 2011) was used to generate gene knock-down mutants. A target fragment was amplified by PCR using KOD-Plus-Neo polymerase and a pair of specific primers (Table 2-1), and inserted at a *Bgl*II site in pSilent-MG.

To obtain fungal transformants with a gene disruption or silencing vector, a PEG-mediated transformation method was used as described previously (Nakayashiki et al., 1999). The resulting fungal transformants having a gene disruption at the desired genomic location or a silencing vector were screened by PCR with appropriate sets of primers for each target gene (Fig. 2-1, Table 2-1).

To construct a gene complementation strain, a genomic DNA fragment containing a target gene and its surrounding region was amplified by PCR with sets of specific primers (Table 2-1) and KOD One (TOYOBO). The PCR product was introduced into the corresponding gene deletion mutant through PEG-mediated co-transformation with the marker plasmid pII99 carrying a geneticin-resistant cassette. Presence or absence of a target gene in the transformants was checked by PCR using a pair of primers (Table 2-1) in the coding sequence (Fig. 2-1).

2.3. Phenotypic characterization of gene knock-out mutants

Every phenotypic assay was performed with three biological replicates unless mentioned otherwise.

Vegetative growth

A mycelial plug was placed at the center of CM agar medium (0.3 % Casamino acids, 0.3% yeast extract, 0.5% sucrose, 0.5% agar) and cultured at 25°C. The colony diameter was measured at 9 days after incubation.

Conidiation, conidial germination, and appressorium formation

Fungal strains were cultured on oatmeal agar media and incubated at 25°C for 7 days, and then, aerial mycelia were removed using the tip of a 1.5 ml microtube. The fungal strains were further cultured under BLB light for 3 days. Conidial suspension was prepared by adding 10ml of distilled water per plate to fungal culture as described previously (Hyon et al., 2012). For germination and appressorium formation assay, 10 µl conidial suspension (1 - 2 x 10^5 conidia/ml) were dropped on a cover glass and incubated at 25°C in the dark under a high humidity condition. Conidial germination was observed after 5 h incubation, and the rate of appressorium formation was counted after 8, 12, 24 h incubation. At least 100 conidia were observed to calculate the rates of conidial germination and appressorium formation in each replicate.

Plant infection assay

Seeds of the wheat cultivar Norin 4 were sown in vermiculite supplied with Hyponex (Hyponex Japan, Osaka, Japan) in plastic seedling pots (5.5 cm × 15 cm × 10 cm), and grown in a plant growth chamber at 23°C with a 12 h-photoperiod for 8 days. Tween 20 (0.01%) was added to conidia suspension, and sprayed onto the adaxial side of the 8-day-old primary wheat leaves. The inoculated seedlings were incubated in a dark and high humidity box for 24 h, and then moved to a plant growth chamber at 23°C with a 12 h-photoperiod

for 4 - 5 days. The disease symptoms were graded by a combination of lesions size (0 to 5) and color (brown [B] or green [G]) as described previously (Hyon et al., 2012). 0, no visible lesion; 1, pinpoints spots; 2, small size (< 1.5 mm); 3, intermediate size (< 3 mm); 4, large and typical blast lesion; 5, whole blighting of leaf blades.

2.4. Cytological assay

Cytological observation was performed as described by Hyon et al. (2012) with a slight modification. The inoculated leaves were collected for observation of appressorium formation at 12 hpi and of infection hyphae in host cells at 24 hpi. The samples were bleached by deeply boiled in alcoholic lactophenol (lactic acid/phenol/glycerol/distilled water/ethanol, 1:1:1:1:8 in volume) at 98^{o}C for 5 minutes. Then, microscopic observation was performed using an epifluorescent microscope under bright and fluorescent fields.

2.5. RNA isolation and qRT-PCR analysis

For RNA extraction, approximately, 50-120 mg of vegetative mycelia, spores or infected leaves were ground to a fine powder in liquid nitrogen with a mortar and pestle. Total RNA was isolated from frozen samples using Sepasol RNA I Super G (Nacalai Tesque, Kyoto, Japan). Total RNA was further cleaned up using the NucleoSpin RNA Clean-up Kit (Macherey-Nagel, Düren, Germany) following manufacture's instruction.

For RT-qPCR analysis, 1 μg of total RNA was subjected to cDNA synthesis using the ReverTra Ace qPCR RT Master Mix with gDNA Remover kit (TOYOBO). RT-qPCR assay was carried out with GeneAce SYBR qPCR Mix α (Nippon Gene, Tokyo, Japan) using pairs of primers listed in Table 1. The actin gene (MGG_03982) was used as an internal control. The level of target mRNA, relative to the mean of the internal control was calculated by the comparative Ct method.

3. Results

3.1. Transcriptional analysis of MoSET1-dependent TFs during plant infection by *P. oryzae*

Among approximately 400 genes that were potentially regulated directly by MoSET1 (Pham et al., 2015a), 18 genes exhibited a typical characteristic of TFs. In this study, we chose 5 of the 18 putative TFs, MGG_00472, MGG_04699, MGG_06898, MGG_07386 and MGG_07450 for functional analysis. First, to gain insight into the functions of these TFs, their gene expression profile at hyphal, conidial and infectious stages was examined by qRT-PCR. At the conidial stage, the mRNA abundance of MGG_04699, MGG_07386 and MGG_07450 was decreased while that of MGG_06898 was significantly increased compared to the hyphal stage (Fig. 2-2). Interestingly, the expression of the MoSET1-dependent TFs was generally increased in infection stages relative to the hyphal stage, especially at an early stage (5 hpi). The abundance of MGG_04699 and MGG_06898 mRNA was increased by approximately 8-fold and 16-fold, respectively, at 5 hpi (Fig. 2-2). In contrast, the mRNA abundance of MGG_07386 was significantly decreased at 5 hpi but increased later at 12 hpi (Fig. 2-2). These results were consistent with the idea that these TFs play roles in the infection process of *P. oryzae.*

3.2. Gene silencing of MGG_00472 and MGG_07386

Despite several trials, we were not able to obtain a gene deletion mutant of MGG_00472 or MGG_07386. This might be due to a lethality of the gene deletion mutants. Indeed, the knock-out mutant of NCU00116, the ortholog of MGG_00472 in *Neurospora crassa*, is maintained only in the form of a heterokaryon (Chen et al., 1998; https://www.fgsc.net/fgsc/strain_detail.php?OrgID=22094). Thus, we decided to use pSilent-MG to analyze the function of MGG_00472 and MGG_07386.

pSilent-MG is a gene silencing vector that triggers retrotransposon-induced gene silencing. In this system, a target gene fragment inserted at a cloning site in the LTR-retrotransposon MAGGY induces both transcriptional and post-transcriptional gene silencing together with the element in *P. oryzae* (Vu et al., 2011).

After initial screening, two candidate transformants each for MGG_00472 or MGG_07386 were subjected to qRT-PCR analysis to assess levels of gene silencing. The candidates showed silencing of the target gene at varying degrees in vegetative mycelia (Fig. 2-3). Consequently, the transformants, KD_mgg00472-12 and KD_mgg07386-13, were selected for further phenotypic analyses.

3.3. Phenotypic characterization of gene knock-out and -down mutants of MoSET1-dependent TFs

Three gene knock-out mutants, Δmgg_04699, Δmgg_06898 and Δmgg_07450, and two knock-down mutants, KD_mgg00472-12 and KD_mgg07386-13 were subjected to phenotypic analyses with respect to growth, sporulation, germination, appressorium formation, and pathogenicity on the host plant.

First, the growth rates of the mutants on rich media (CM agar media) were assessed. Δmgg_04699, Δmgg_06898, and KD_mgg00472-12 showed a slower growth while, interestingly, the growth rate of KD_mgg07386-13 was a little faster than the WT strain (Fig. 2-4a).

With an exception of Δmgg_07450, all the mutant examined displayed a decrease in conidiation compared to WT at varying degrees (Fig. 2-4b). Especially, Δmgg_06898 produced almost no conidia, suggesting that MGG_06898 plays a crucial role in conidiogenesis in *P. oryzae*. Meanwhile, due to this, further phenotypic assays that use conidia were not applicable to Δmgg_06898.

The rates of germination and appressorium formation were assessed using conidial suspension dropped on a cover glass. The conidia were incubated in the dark at 25°C up to 24h. The germination rates of the mutants did not differ much from that of WT except that Δmgg_04699 exhibited a rate less than 60% relative to WT (Fig 2-4c). In addition, only Δmgg_04699 showed a deficiency in appressorium formation. At 12 hpi, 22% of conidia formed an appressorium in Δmgg_04699 while more than 85% of conidia did it in the WT and other mutant strains (Fig. 2-4d). The deficiency of Δmgg_04699 in germination and appressorium formation was restored to the WT levels in the gene complementation strain, indicating that MGG_04699 is responsible for the phenotypic alterations in the mutant.

In infection assay, KD_mgg00472-12 and Δmgg_04699 showed significantly reduced virulence on the host plant (Fig. 2-5a). The infection types of KD_mgg00472-12 and Δmgg_04699 were 3-4BG and 2-3BG, respectively. Cytological observation of infected leaves indicated that both KD_mgg00472-12 and Δmgg_04699 exhibited a delay in invasion to plant cells compared to WT. At 24 hpi, the rates of appressoria that successfully formed infection hyphae in the host cell were 45% and 31% with KD_mgg00472-12 and Δmgg_04699, respectively, while that with WT were approximately 80% (Fig. 2-5b). These results suggested that MGG_00472 and MGG_04699 contributed to the full virulence of *P. oryzae* by regulating their downstream genes.

The infection type of KD_mgg07386-13 was 5B. Lesions appeared in almost the whole leave (Fig. 2-5a). However, in contrast to leaves infected with the WT strain, the color of lesions was mostly brown, indicating that this mutant induced more resistant reaction than did the WT strain. Thus, MGG_07386 may be required for suppressing a part of resistant reactions by the host plant.

4. Discussions

Among the MoSET1-dependent TFs examined in this study, MGG_00472 and MGG_04699 considerably contributed to the virulence of *P. oryzae*. MGG_04699 named as MoFLBC (Cao et al., 2016) is a homolog of FlbC, C2H2 transcription factor in *Aspergillus nidulans* (Kwon et al., 2010). FlbC is necessary for conidiation, conidial germination and, proper development in *A. nidulans*. Possible orthologs of FlbC were present in a wide range of fungal species. In *Fusarium verticillioides*, the FlbC ortholog negatively regulated the production of conidia (Malapi-Wight et al., 2014). More recently, Boni et al. (2018) reported that FLB-3, an ortholog of FlbC in *Neurospora crassa*, was essential for fungal development. Thus, FlbC homologs play roles in regulating various stages of fungal development in a wide range of ascomycetes.

In *P. oryzae*, Cao et al. (2016) showed that a deletion mutant of MGG_04699 had a severe defect in sporulation and its virulence to the host plant as shown in this study. However, contrary to our study, the rates of germination and appressorium formation were 96.9% and 94.9%, respectively, relative to WT in their study. This apparent discrepancy may be due to a difference in the strains and/or experimental conditions.

To date, MGG_00472 as well as MGG_07386 and MGG_07450, have not been well-characterized in *P. oryzae*. MGG_00472 is an ortholog of the *Aab-1* gene (NCU00116) encoding a CCAAT-binding TF subunit. *Aab-1* was reported to regulate a glutamate dehydrogenase gene and have pleiotropic effects on growth and development (Chen et al., 1998). Consistently, KD_mgg00472-12 showed defects in growth, sporulation, and virulence to the host plant. Thus, MGG_00472 may also have pleiotropic effects on growth and development in *P. oryzae*. Possible orthologs of MGG_07386 and

MGG_07450 were conserved in ascomycete fungi but their biological functions were so far not well-understood.

MGG_06898, namely MoMyb1, encodes a TF belonging to the Myb protein family. Consistent with our results, Dong et al. (2015) previously revealed that a deletion mutant of MoMyb1 showed defects in vegetative growth, conidiation and conidiophore development. In the MoMyb1 deletion mutant, several conidiogenesis-related genes such as MoMSN2, MoFlbC (MGG_04699), MoGLUS, MoSTUA, and MoCON8 were significantly down-regulated (Dong et al., 2015). Thus, MoSET1-dependent MoMyb1 plays a key role in conidiogenesis.

Based on the literatures and this work, at least fifteen MoSET1-dependent TF genes in *P. oryzae* have been characterized to date, which includes MGG_00472, MGG_07386, MGG_07450, MGG_01414 (Xlr1), MGG_01518 (MoNIT4), MGG_01486 (FZC2), MGG_02880 (FZC9), MGG_04699 (MoFLBC), MGG_06898 (MoMyb1), MGG_08199 (FAR2), MGG_09200 (TDG1), MGG_09950 (FZC54), MGG_00617 (MoVOSA), MGG_01734, and MGG_13778 (MoGIS2) (Kim et al., 2014; Lu et al., 2014; Dong et al., 2015; Cao et al., 2016). Among those, 3 (MGG_00472, MGG_06898, MGG_09950), 10 (MGG_00472, MGG_01518, MGG_01486, MGG_02880, MGG_04699, MGG_06898, MGG_08199, MGG_09200, MGG_01734, MGG_07386), 2 (MGG_01486, MGG_04699), and 4 (MGG_00472, MGG_04699, MGG_09200, MGG_13778) TFs were shown to play a role in vegetative growth, sporulation, appressorium formation and virulence to the host plant, respectively (Fig. 2-6). Thus, MoSET1 may function as a key regulator of the pathogenicity of *P. oryzae* by controlling TFs that further regulate various steps in the infection process such as sporulation, appressorium formation, and invasion to the host cell.

Table 2-1. Primers used in this chapter

Primer	Sequences
MoActin F	5’-GCGGTTACACCTCTCTACCAC-3’
MoActin R	5’-AGTCTGGATCTCCTGCTCAAAG-3’
HY F	5’-CGTTGCAAGACCTGCCTGAA-3’
YH R	5’-GGATGCCTCCGCTCGAAGTA-3’
MGG_00494_up F	5’-CTGTGGGTTTTTCTGCACCT-3’
MGG_00494_up R	5’-CAAGCTGGAAATGTTGCTCA-3’
MGG_00494_dn F	5’-CAAAGGGCTGGGATTACCTT-3’
MGG_00494_dn R	5’-CAAGCTGGAAATGTTGCTCA-3’
MGG_00494_check F	5’-GCTACACCCCGACTTCATGT-3’
MGG_00494_check R	5’-GGCTCAGCGAACCATTAGAG-3’
MGG_04699_up F	5’-ACGTATCCCACCACACATCATC-3’
MGG_04699_up R	5’-AGGGTTCGTGATACCGATTTGT-3’
MGG_04699_dn F	5’-ACGAACCGAAACGACATAGACT-3’
MGG_04699_dn R	5’-CTTATTTGTTCGCCCGTTACCC-3’
MGG_04699_check F	5’-CTTGTGTACCTTGCGATGTCTG-3’
MGG_04699_check R	5’-ACTTTAGAGCTGAATTGGCCCA-3’

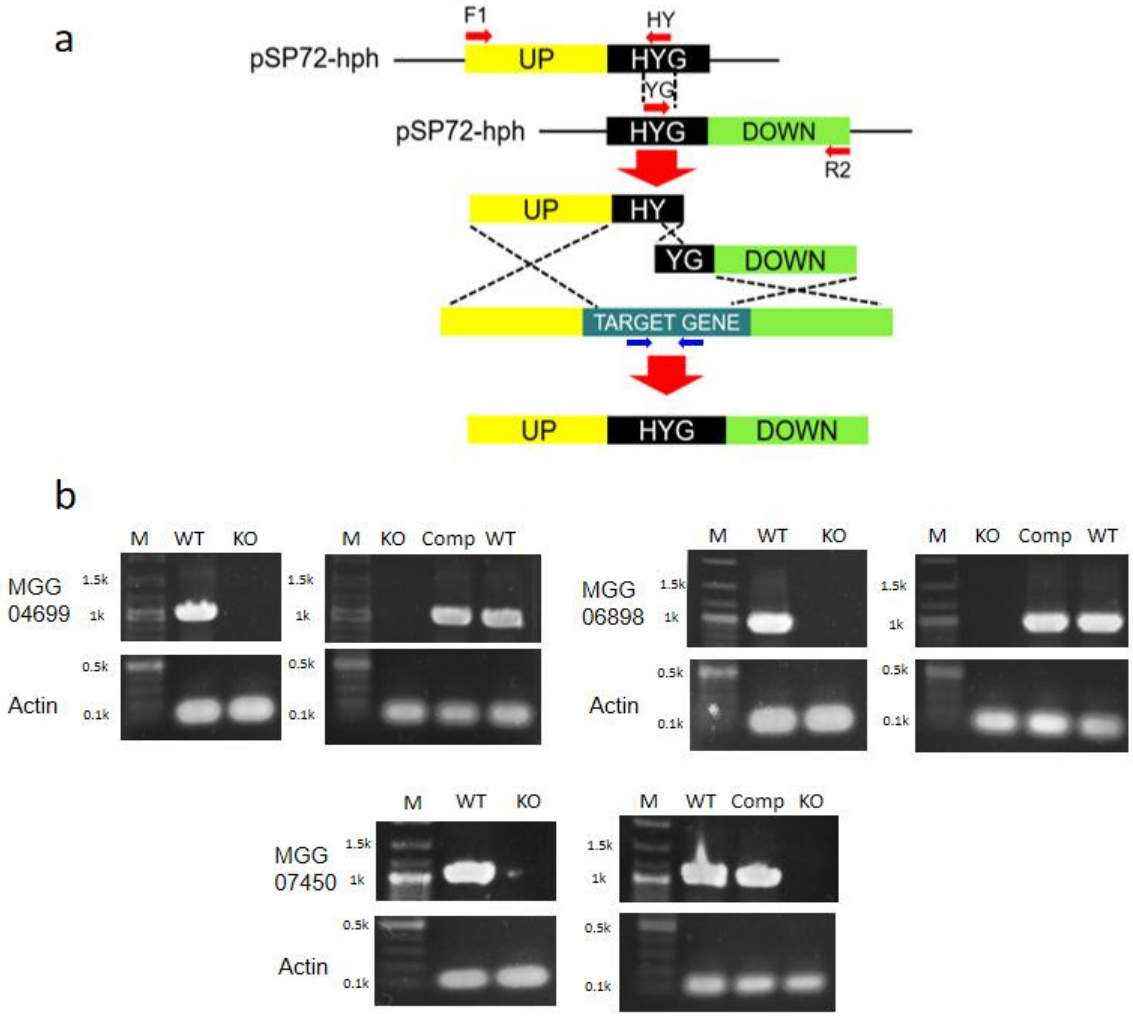

Fig 2-1. Construction of gene knock-out mutants

a, Diagram of a split-marker strategy for gene disruption. Up- and down-stream flanking regions of a target gene were amplified by PCR and cloned into pSP72-hph individually. Using the resulting plasmids as templates, DNA fragments containing a part of the hygromycin resistant gene (HYG) and the flanking regions were amplified by PCR as shown above. By introducing the resulting PCR fragments into *P. oryzae*, the target gene was replaced with the HYG gene by homologous recombination. **b,** Screening of knock-out mutants and gene complementation strains. Presence or absence of a target gene was checked by PCR using a pair of primers (Table 2-1) in the coding sequence (indicated by blue arrows in **a**). As a control, a fragment of the actin gene was amplified to verify genomic DNA template. M, molecular marker; WT, wild-type strain (Br48); KO, knock-out mutant; Comp, gene complementation strain.

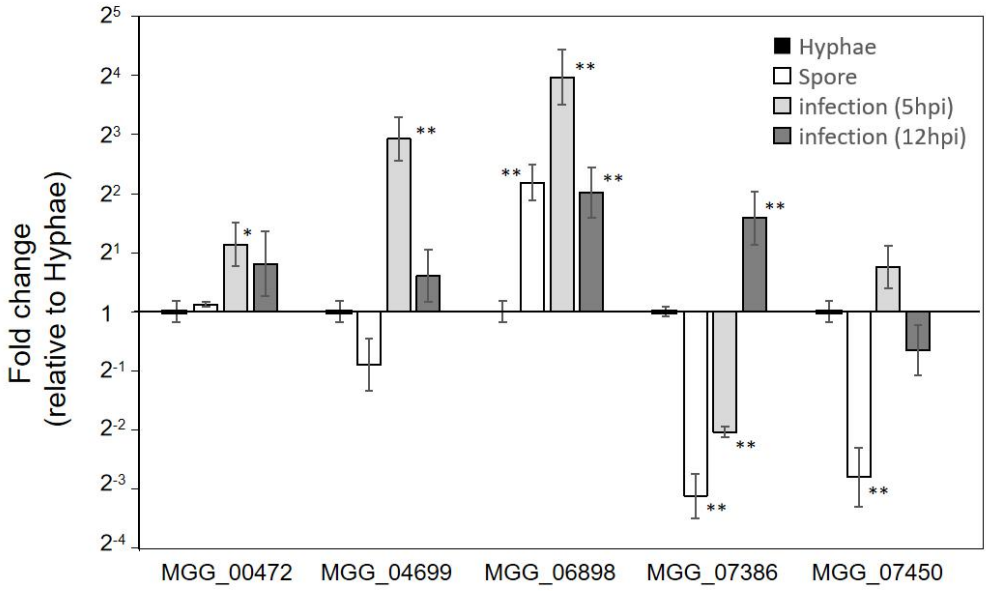

Figure 2-2. Quantitative RT-PCR analysis of five MoSET1-dependent transcription factors at hyphal, conidial and infectious stages in P. oryzae. Actin was used to normalize mRNA expression level. Data show fold change (relative to mRNA quantity in hyphae) ±standard error (n = 3). Asterisks are given to indicate significant difference at $p < 0.05$ (*) and $p < 0.01$ (**) (two-tailed t-test).

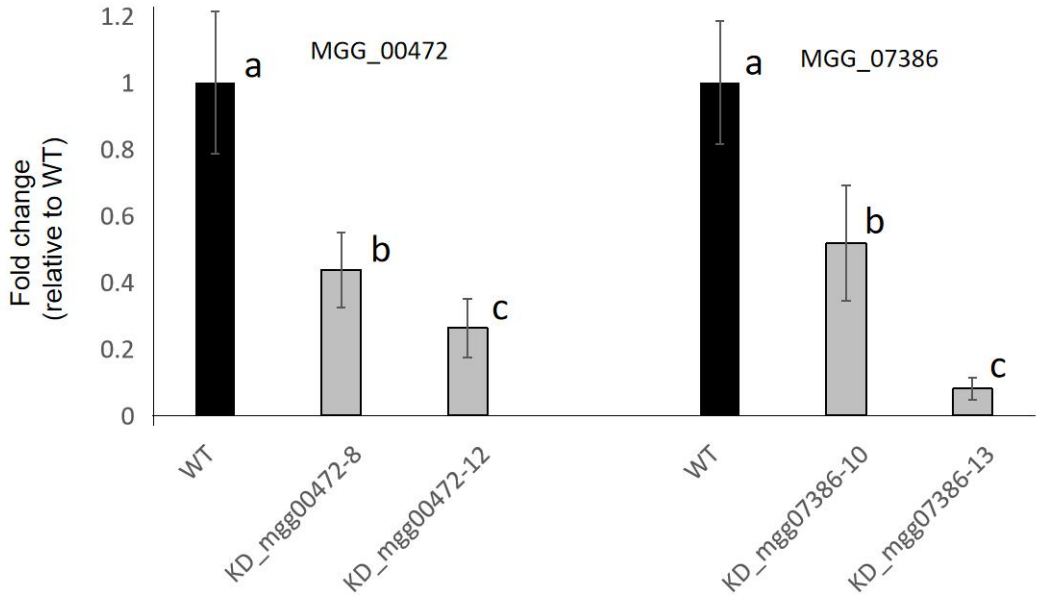

Figure 2-3. Quantitative RT-PCR analysis of MGG_00472 and MGG_07386 mRNA in candidates of their knock-down mutants. Actin was used to normalize mRNA expression level. Data show fold change (relative to mRNA quantity in the wild-type strain) ±standard error (n = 3). a-c, Different characters indicate significant differences by Tukey's HSD ($P < 0.05$).

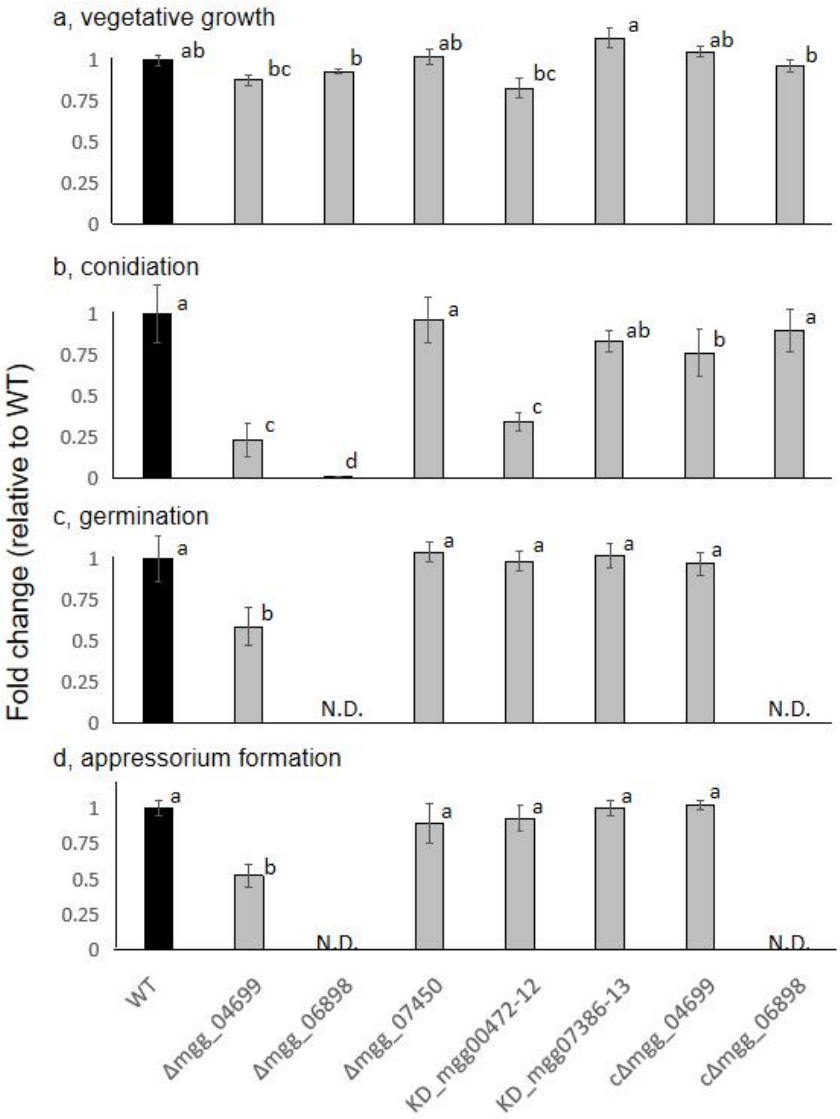

Figure 2-4. Phenotypic characterization of knock-out and -down mutants of MoSET1-dependent TFs in *P. oryzae.* a, Diameters of fungal colonies were measured at 9 days after inoculation on rich agar medium. b, Conidiation was evaluated by counting the number of conidia under a light microscopy as described in details in Materials and method. c-d, The rates of conidial germination (c) and appressorium formation (d) were measured by observing conidial suspension on hydrophobic surface under a light microscope after 5 h (conidial germination) and 24 h (appressorium formation) incubation at 25℃.
Black bars indicate the wild-type strain Br48 (WT) and grey bars represent knock-out and –down mutants of MoSET1-dependent TFs and their gene complemented strains (cΔmgg_04699 and cΔmgg_06898). Data show fold change (relative to the wild-type strain) ±standard error (n = 3). a-d, Different characters in the graphs indicate significant differences by Tukey's HSD ($P < 0.05$). ND, not determined.

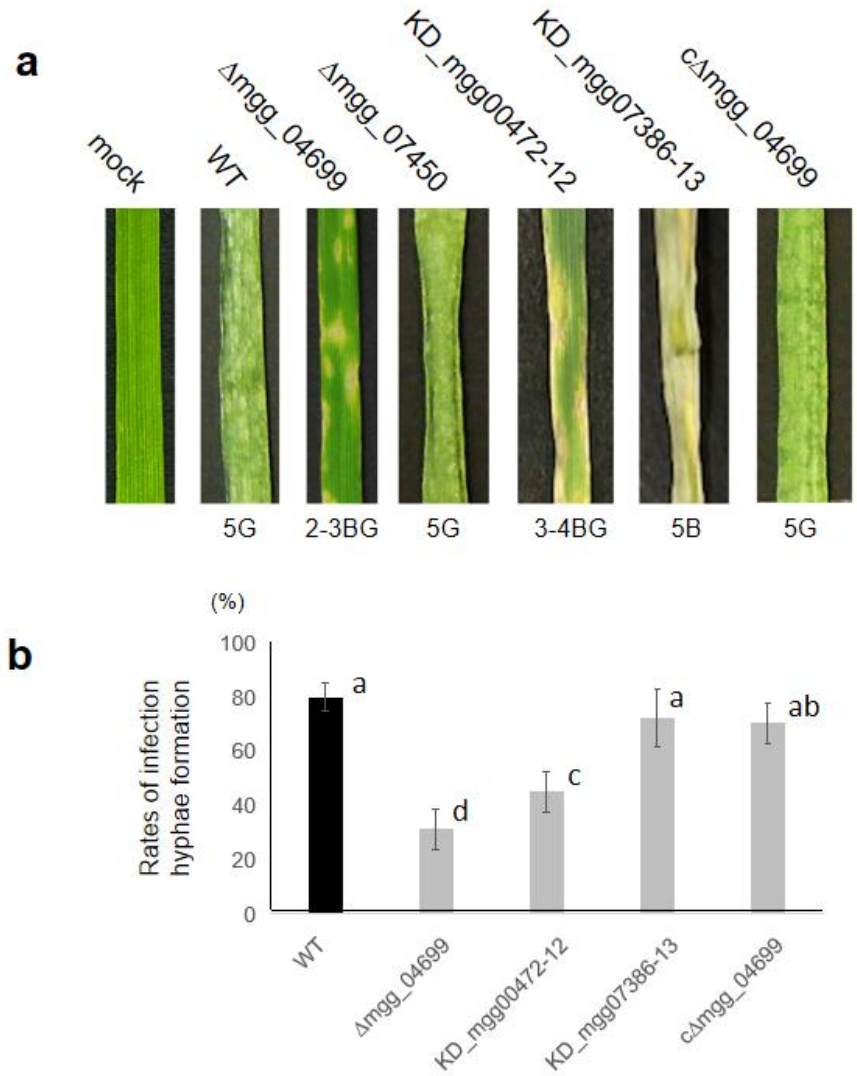

Figure 2-5. Inoculation test of knock-out and -down mutants of MoSET1-dependent TFs in P. oryzae. a, Infection assay was performed on the wheat cultivar Norin 4 at 23℃. Four to five days after inoculation, symptoms on the inoculated plants were evaluated. Letters under pictures of infected leaves indicate disease index values by a grading method (Hyon et al., 2012). This experiment was repeated at least three times, and representative samples are presented. **b,** The rates of infection hyphae formation in infected leaves. The black bar indicates the wild-type strain Br48 (WT) and grey bars represent knock-out and –down mutants of MoSET1-dependent TFs and a gene complemented strain (cΔmgg_04699). Error bars represent standard errors of the mean (n = 10). a-d, Different characters in the graph indicate significant differences by Tukey's HSD ($P < 0.05$).

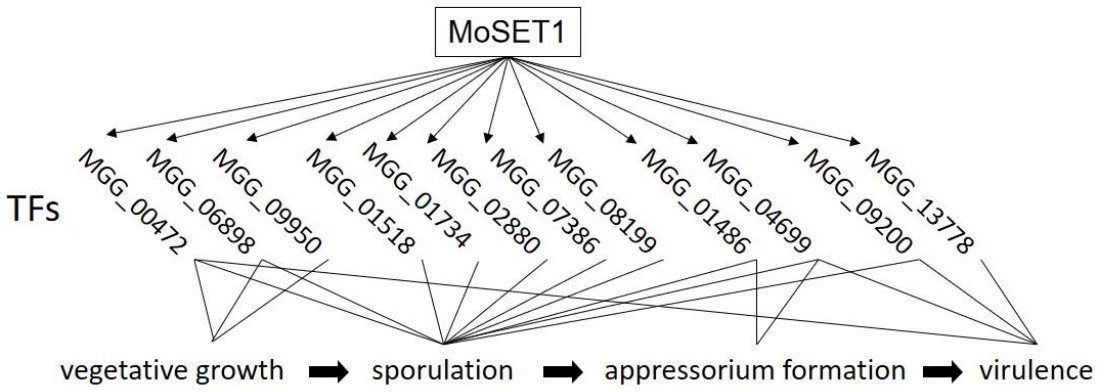

Figure 2-6. Schematic diagram of putative MoSET1 regulatory network during infection-related morphogenesis in *P. oryzae*.

CHAPTER III

ROLES OF RNA SILENCING COMPONENTS IN PATHOGENESITY IN *P. ORYZAE*

1. Introduction

Recent studies have been shown that RNAi is involved and plays an important role in fungal pathogenicity. RNAi is used not only to preserve the integrity of the genome but also to respond to environmental stress and is also an important factor to support the fungus entering the host as well as enhance the virulence of the fungus (Weiberg et al., 2013; Qutob, 2013; Torres-Martínez et al., 2017; Hua et al., 2018). In the highly virulent pathotype isolate T2, the high expression levels of all six V. nonalfalfae RNAi genes were observed (Jeseničnik et al., 2019).

Active RNAi pathways in *Colletotrichum gloeosporioides* or *M. oryzae* enhancing the pathogenicity whereas the lacking one or two RNAi genes in those species showed a significant decrease in the virulence (Wang et al., 2018; Raman et al., 2017). Similarly, the severe decrease in virulence appear in the white mold fungus *Sclerotinia sclerotiorum* strain which lack of RNAi components such as Δ*ago2* mutant (Neupane et al., 2019) and Δ*dcr1*/*dcr2* double mutant (Mochama et al., 2018).

Here we showed that RNAi mutants showed variable levels of defects in vegetative development, sporulation, appressorium formation and pathogenicity in *P. oryzae*. Especially in this fungus the MoDCL genes were important for the formation of appressorium and infection-related growth.

2. Materials and methods

2.1. Fungal strains

The *P. oryzae* wild-type strain Br48 (Urashima et al., 1999) was stored on barley seeds soaked with sucrose 0.5% solution, after being dried in a plastic container with silica gel at 4^{o}C for long-time period storage (Nakayashiki et al., 1999). A barley grain from the stock culture was placed on a PDA (potato

dextrose agar) plate and incubated at 25°C for the working culture of fungi. *P. oryzae* was grown in CM broth (0.3% yeast extract, 0.3% amino acids, 0.5% sucrose) at 25°C for DNA isolation and protoplast preparation (Kieu et al., 2014).

2.2. Construction of gene knock-out mutants of RNAi components

To construct a double dcl mutant (Δdcl1/2), we use the Δdcl1 strain as a parental strain (Kadotani et al., 2004). Similarly, Δrdrp1/3, a double knock-out mutant of MoRdRP1 and MoRdRP3 was first constructed by a conventional gene disruption method to serve as a parent strain for a triple knock-out mutant of MoRdRP1, MoRdRP2, and MoRdRP3. The primers used for the construction of gene disruption vectors were shown in Table 3-1.

2.3. Protoplast preparation and transformation

P. oryzae was grown in CM liquid for protoplast preparation for 4 days at 25°C on a 100 rpm shaker. Digested fungal cell walls by shaking in solution with 10mg/ml lysing enzymes (Sigma). As previously described, the upstream and downstream PCR fragments of the target gene were combined with a drug resistance gene, and introduced into fungal protoplasts by a polyethylene glycol (PEG)-mediated method (Kadotani et.al., 2003). 200µl protoplast suspension was mixed with 10µg plasmids DNA and 3µg of a plasmid carrying a geneticin or hygromycin resistance gene cassette. After 10 minutes of incubation on ice, 200µl, 400µl, 800µl PEG was added in a step-by -step manner. Then PEG solution was removed after centrifugation at 5000rpm for 10 minutes. After mixing with 30ml of CM 20% sucrose media (0.3% yeast extract, 0.3% casamino acids, 20% sucrose, 1.5% agar), protoplasts were resuspended in 1ml of STC solution and poured into two plastic dishes. CM media containing 400µg/ml of geneticin or hygromycin was overlaid to the plates after 24h incubation, and incubated at 25°C for 5-7 days. Transformants were moved to new PDA (Potatoes Dextrose Agar) dishes for screening. For

the screening of transformants, PCR was conducted by a fungal colony PCR method with suitable sets of primers for each gene.

2.4. Plant materials, assays for growth rate, conidiation, conidial germination and appresorium formation and infection tests

The wheat cultivar, *T. aestivum* "Norin 4", and two barley cultivars S615 and Bar14 Nigrate were used. S615 was resistant but Bar14 was super-susceptible to Br48 (Hyon et al., 2012). Norin 4 was susceptible to Br48 (Zhan et al., 2008; Hyon et al., 2012).

Assays for growth rate, conidiation, conidial germination, appressorium formation and plant infection tests were performed as described in Chapter II.

3. Results

3.1. MoDCL1/2 deletion mutants show defects in infection-related morphogenesis

To test the role of the different RNAi components in vegetative hyphal growth, Δdcl1/2 and Δrdrp1/2/3 were cultured on CM (0.5% sucrose) media and their colony diameters were measured. The growth rate of double Δdcl1/2 mutants was significantly lower than that of the wild type and Δrdrp1/2/3 strain (Fig. 3-3). These results suggested that DCLs contributed to hyphal growth. In contrast, Δrdrp1/2/3 mutants grew as efficiently as did the wild-type strain on the rich media.

The rates of conidiation, germination, appressorium formation, and pathogenicity on host plants were evaluated for the Δrdrp1/2/3 and Δdcl1/2 mutants together with the wild-type strain. The most severe defect was observed in the conidiation of the Δdcl1/2 mutant. Compared with the wild-type strain, the rates of conidiation were reduced by 82% in the Δdcl1/2 mutants. In contrast, neither Δdcl1/2 nor Δrdrp1/2/3 exhibited defects in germination and appressorium formation (Table 3-1). The rates of

germination were 86.78%, 87.22%, 86.67% in the wild type, Δdcl1/2 and Δrdrp1/2/3 mutants, respectively (Table 3-1). Intriguingly, the appressorium formation was reduced in the Δdcl1/2 mutants (90.22%) compared with the wild-type (94.89%) (t-test, $p<0.05$), while the Δrdrp1/2/3 mutants (92.89%) was also slightly decrease compared with the wild-type but there was no statistically significant difference (t-test, $p<0.05$). This suggested the lacking of both dcl genes impaired the formation of appressorium in *P. oryzae*.

These findings showed that DCL genes play a significant role in conidial development, which may result in a reduction in the pathogenicity of the fungus.

3.2. *P. oryzae* RNA silencing components deletion mutants show defects in pathogenicity on host plants

I performed infection assays using wheat and barley cultivars with different degrees of resistance/susceptibility to the wheat blast fungus Br48 to examine the functions of RNA silencing components during infection. The order of susceptibility of the host plants to Br48is as follows: Nigrate Bar14 (barley, super susceptible) > Nakazumi-zairai Norin 4 (wheat, susceptible) > S615 (wheat, resistant). Seedlings of the wheat and barley cultivars were inoculated with conidia of Br48, Δdcl1, Δdcl2, Δddcl1/2, Δrdrp1, Δrdrp2, Δrdrp3, and Δrdrp1/2/3 (Fig. 3-5). Δdcl1/2 mutants showed a considerable reduction in the pathogenicity on both Bar14 and Norin 4. Δdcl1/2 mutants produced only a few lesions graded as 1-2BGy while the infection types of Δdcl1, Δdcl2, Δrdrp1, Δrdrp2, Δrdrp3, Δrdrp1/2/3, and Br48 were 2-3BGy, 2-3BGy, 3BGy, 3BGy, 3BGy, 3BGy, and 3BGy, respectively, on Norin 4. On Bar14, the infection type of Δdcl1/2 mutants was less severe whereas those of the other strains tested were all 5G. These results indicated that Dicer enzyme

activity either from MoDCL1 or MoDCL2 is necessary for the cell growth of *P. oryzae* and its full virulence on host plants.

4. Discussion

The Dicer proteins play an important role in regulating the production of sRNAs in eukaryotes. Many pieces of evidence demonstrated the role of Dicer protein in the growth, conidiation, and pathogenicity of the pathogen. Yin C et al (2020) found that silencing Dicer-like genes in *Penicillium italicum* resulted in a reduction in sRNA biogenesis and also in the virulence of the fungus in citrus fruits. The research also suggested that sRNA may be trafficking from *P. italicum* to citrus fruits to suppress the expression of host genes, which is termed cross-kingdom RNAi. Wang (2017) also showed that the growth, conidiation, and the pathogenicity of *Colletotrichum gloeosporioides* were regulated by Dicer-like proteins. In *P. oryzae*, Raman et al. (2017) showed that sRNA was required for the growth and development of the fungus where loss of a single gene encoding Dicer, RNA-dependent RNA polymerase, or Argonaute caused a reduction in conidiation, and especially that of MoRdRP1 and MoAGO3 resulted in a significant decrease in growth and virulence on a host plant. Similarly in *Fusarium graminearum,* RNAi components were reported to be involved in sexual and asexual multiplication, and pathogenicity (Gaffar, 2019).

In some cases, molecular mechanisms of cross-kingdom RNAi were unveiled. For instance, Vm-milRNAs, miRNA-like RNAs in *Valsa mali*, contribute to the successful infection of the fungus on apple trees by adaptively regulating virulence genes (Ming Xu, 2020). Similarly, Cui (2019) showed that the pathogenic fungus *Beauveria bassiana* exports a microRNA-like RNA (bba-milR1) that hijacks the host RNA-interference machinery in mosquito cells by binding to Argonaute 1. bba-milR1 is highly

expressed during fungal penetration of the mosquito integument, and suppresses host immunity by silencing the expression of the mosquito Toll receptor ligand Spätzle 4 (Spz4).

By sequencing sRNAs produced by *Sclerotinia sclerotiorum* in vegetative mycelia and at some stage in infection of host species, *Arabidopsis thaliana* and *Phaseolus vulgaris*, Derbyshire et al. (2019) discovered that *S. sclerotiorum* produces at the least 374 distinct incredibly plentiful sRNAs during infection, mostly originating from repeat-rich plastic genomic regions. Some of the sRNA seemed to target host genes for silencing during infection. Consistently, *A. thaliana* mutants of SERK2 and SNAK2, possible sRNA target genes, showed greater susceptibility to *S. sclerotiorum.* Thus, *S. sclerotiorum* sRNAs may also make contributions to the silencing of immune components in host plants.

Recent studies have revealed bidirectional cross-kingdom conversation of sRNAs among host plants and adapted fungal pathogens.

Weiberg et al. (2013) showed that the host plant immune system is perturbed by sRNA exported from *B. cinerea*. In turn, plants export natural or exogenous synthetic sRNAs to suppress fungal gene expression. Zhang et al. (2016) demonstrated that cotton plants export miRNAs to inhibit fungal virulence genes.

My findings indicated that Dicer-like proteins in *P. oryzae* play a role in hyphal growth, conidial development, and virulence of the fungus. However, there are still several important unanswered questions, what kind of sRNA processed by Dicer contributes to fungal pathogenicity and how do they work to encounter the host plant? As a first step to address these questions, I perform a deep sequencing analysis of sRNA in *P. oryzae* in the next chapter.

Tables and figures

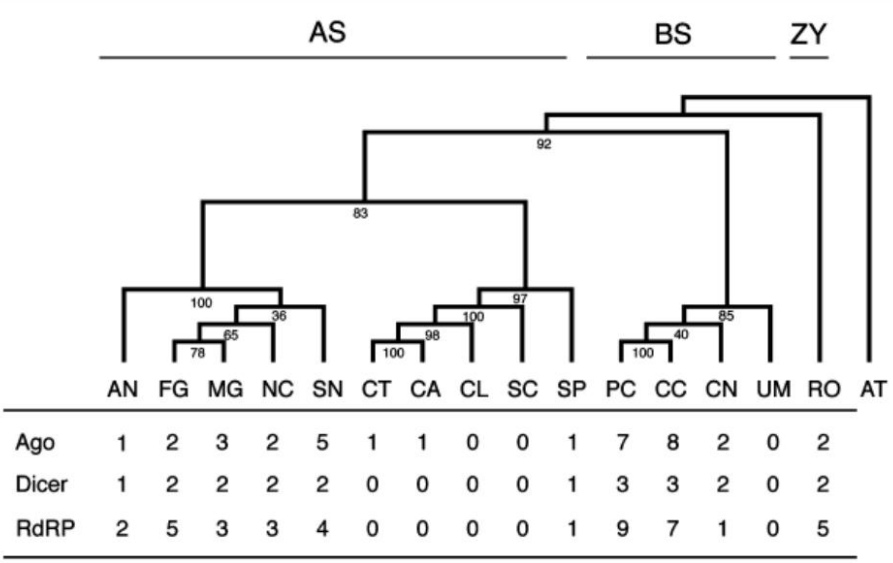

Figure 3-1. Phylogenetic relationship of some fungal species based on ß-tubulin sequences and the numbers of Ago, Dicer, and RNA-dependent RNA polymerase (RdRP)-like proteins found in their genomes. Arabidopsis was used as an outgroup to root the tree. AS, ascomycetes; BS, basidiomycetes; ZY, zygomycete; AN, *Aspergillus nidulans*; CA, *Candida albicans;* CC, *Coprinus cinereus*; CL, *Candida lusitaniae*; CN, *Cryptococcus neoformans*; CT, *Candida tropicalis*; FG, *Fusarium graminearum*; MG, *Magnaporthe oryzae (grisea)*; NC, *Neurospora crassa*; PC, *Phanerochaete chrysosporium*; RO, *Rhizopus oryzae*; SC, *Saccharomyces cerevisiae*; SN, *Stagonospora nodorum*; SP, *Schizosaccharomyces pombe*; UM, *Ustilago maydis*; AT, *Arabidopsis thaliana* (Nakayashiki et al., 2006).

A

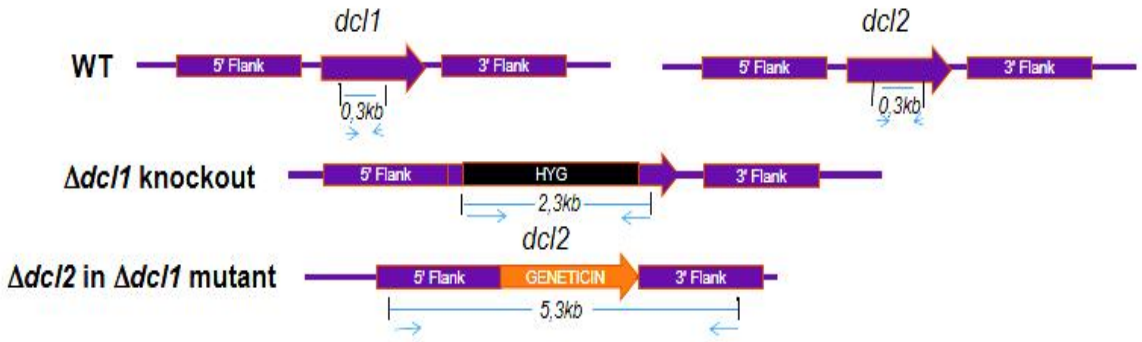

B

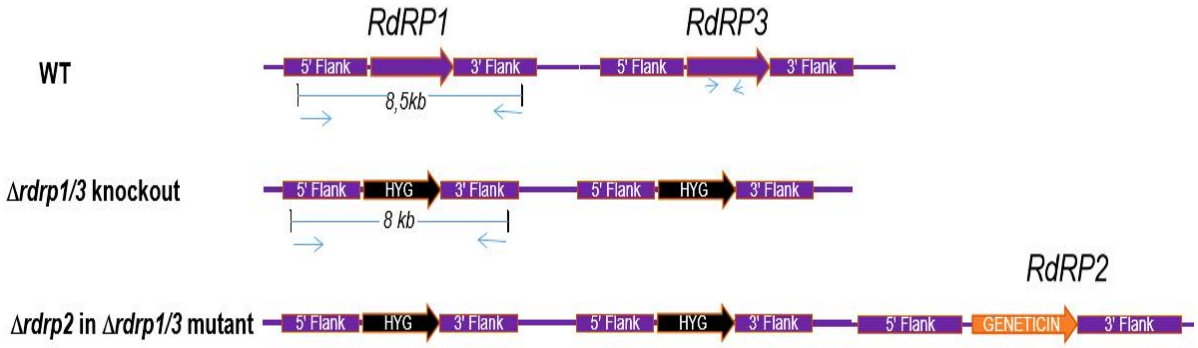

Figure 3-2. Construction of dcl1/2 and rdrp1/2/3 deletion strains. **A**, Gene structure of DCL alleles with introns (lines) and exons (boxes). Deletion was constructed by using the split-marker system. To make double dcl mutant (Δdcl1/2) we use Δdcl1 strain as parental strain and make dcl2 mutant to get double dcl mutant. **B**, Gene structure of RdRP alleles with introns (lines) and exons (boxes). Make double mutant Δrdrp1/3 by transforming rdrp1 and rdrp3 disruption materials (both of them containing hygromicin resistantce gene) at the same time, then use Δrdrp1/rdrp3 as parental strain and make rdrp2 mutant (containing geneticin resistantce gene) to get triple rdrp mutant (Δrdrp1/2/3).

A

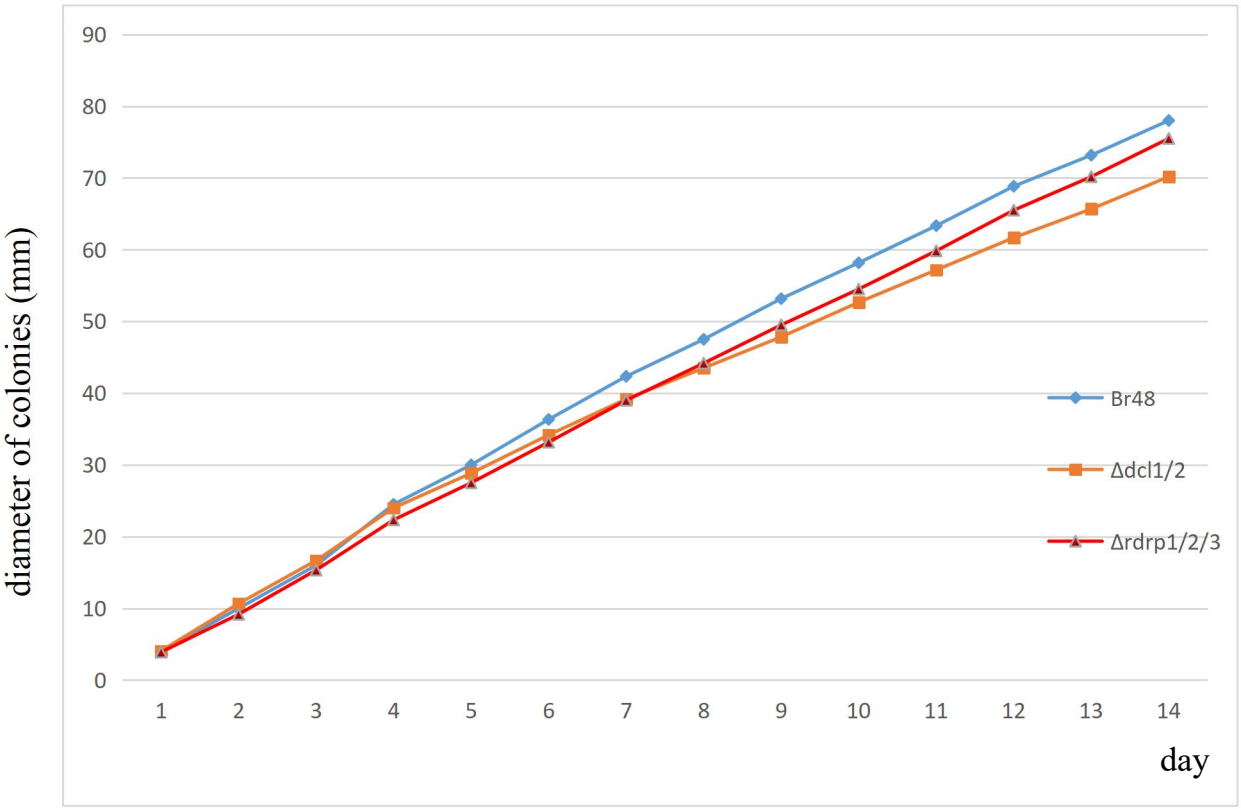

B

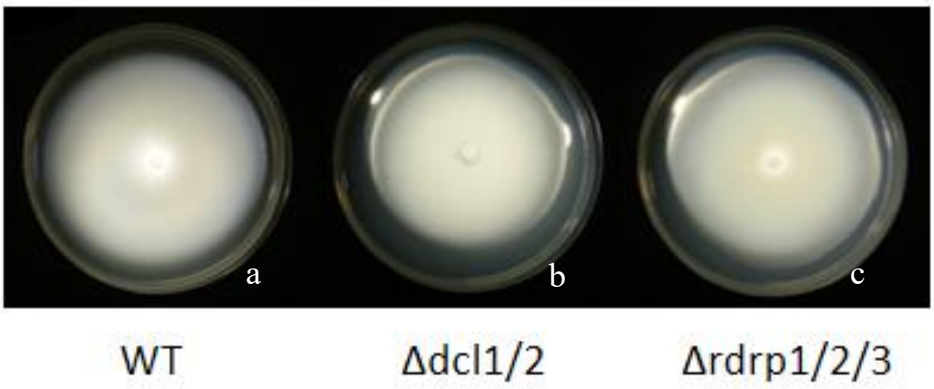

Figure 3-3. Growth rate of the *dcl and rdrp* mutants of *M. oryzae*. (**A**) Vegetative growth was measured for 14 days on PDA medium. The graphs show average of three independent replications. (**B**) Mycelium growth at 14 days after incubation at 25°C; (a) Wild type Br48 strain, (b) *⊿dcl1/2*, (c) *⊿rdrp1/2/3*

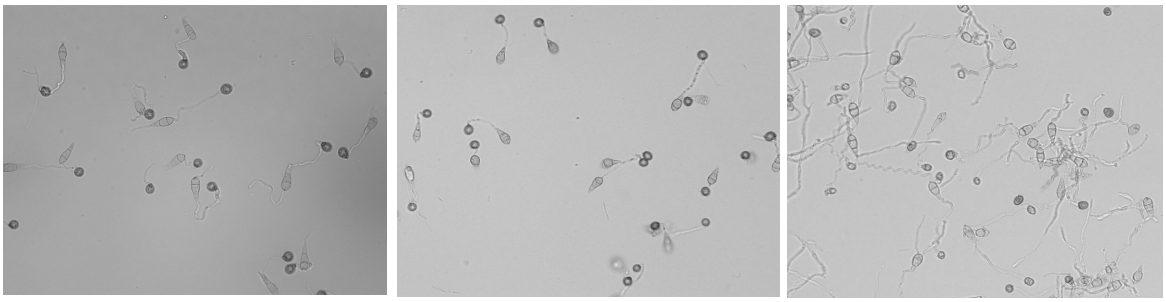

WT *△dcl1/2* *△rdrp1/2/3*

Figure 3-4. Effect of *dcl and rdrp* deletion on appressorium formation. Δrdrp1/2/3 mutants have appressorium formation at 94.89% and 92.89% respectively at levels comparable to the wild-type, the rate of Δdcl1/2 mutants decreases slightly to 90.22%. Both DCL genes play a significant role in the development of appressorium.

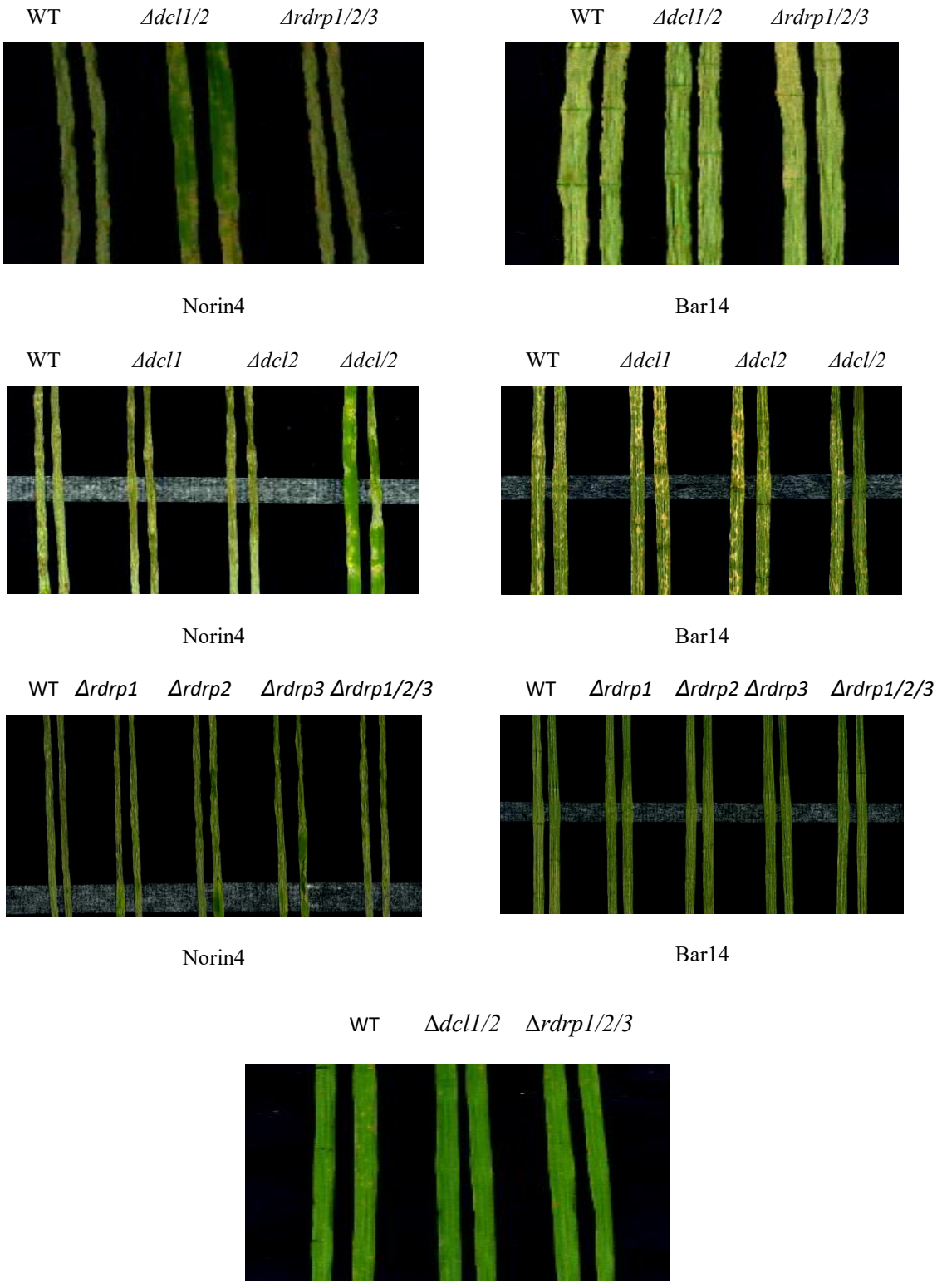

Figure 3-5. Infection assays of the *dcl and rdrp* deletion mutants. Infection assay was performed on the wheat cultivar Norin 4, Bar 14 and S615. Four to five days after inoculation, symptoms on the inoculated plants were evaluated by a grading method. This experiment was repeated at least three times, and representative samples are presented.

Table 3-1. Comparison of phenotypes among mutants and wild type

Strain	Mycelial growth on CM (14 days, mm)	Conidiation (10ml suspension)	Germination (%)	Appressorium formation (%)
WT	78	65.44	86.78	94.89
Δ*dcl1/2*	70.17*	10.89**	87.22	90.22
Δ*rdrp1/2/3*	75.5	59.44	86.67	92.89

Asterisks are given to indicate significant difference at $p< 0.05$ (*) and $p< 0.01$ (**) (one-tailed t-test).

Table 3-2. List of primers used in this chapter

RNAi primer	sequence
MoDcl2Up-F	*5′-TTACCTGAAGTCATTACCGCCC-3′*
MoDcl2Up-R	*5′-GGGTTCATTGCAACTGACCTTC-3′*
MoDcl2Dn-F	*5′-TTTGATCCAGACGTGACCATGT-3′*
MoDlc2Dn-R	*5′- CACCACGCTCCACAAAATCATT-3′*
MoDcl2-F (496F)	*5′-TGGACTGATCAACGAACATC-3′*
MoDcl2-R (497R)	*5′-GAAACTAGGGTCTGTACTAC-3′*
MDL1-F	*5′-AGCTGACTGGCTGATTGGTG-3′*
MDL1-R	*5′-GT-CACGCATTTTCTGCTCGTTG-3′*
MoDcl1-F (489F)	*5′-AGCTGACTGGCTGATTGGTG-3′*
MoDcl1-R (490R)	*5′-GTCACGCATTTTCTGCTCGTTG-3′*
Mo*RdRp1* Up-F	*5′-CCCCTCGAGCAGTATGCAATGGTGTGTTGC-3′*
Mo*RdRp1* Up-R	*5′*-CCCCTCGAGAGGACTTGACATGTTCCTTGC*-3′*
Mo*RdRp1* Dn-F	*5′*-CTAGAAAAAGGTACAGGCGAGATG-*3′*
Mo*RdRp1* Dn-R	*5′*-GTACTCGTTTGGGTTGACGAAG-*3′*
MoRdRp2 Up-F	*5′*-CACTCTCAAGCTTGCAGTCATT-*3′*
MoRdRp2 Up-R	*5′*-TGACTCGAAGTAGTTTGGTGATGT-*3′*
MoRdRp2 Dn-F	*5′*-GTAAATCTAACCTTCCCTGCTTGA-*3′*
MoRdRp2 Dn-R	*5′*-TACAAAAACACACCTTTTCGGCTA-*3′*
MoRdRp3 Up-F	*5′*-CCCCTCGAGTGTCAGCGACAGACTTGGAG-*3′*
MoRdRp3 Up-R	*5′*-CCCCTCGAGAGGTAAGGCACGTTCCAACA-*3′*
MoRdRp3 Dn-F	*5′*-GAGCTCTCATCGGGGCTATTCTCAAC-*3′*
MoRdRp3 Dn-R	*5′*-GAGCTCCAATGCGGTCAACCTGAGTA-*3′*
MoRdrp1-F	*5′*-CTGGTTATCTCTTCACCCGGAC-*3′*
MoRdrp1-R	*5′*-TGGTCGTTGAGTAAAGTACCGG-*3′*
MoRdrp2-F	*5′*-GAAAGTATGTTGGCAGAGCAGC-*3′*
MoRdrp2-R	*5′*-TGAGCTTTCTTGCCTCTCTGAG-*3′*
MoRdrp3-F	*5′*-CTCAACCGTGGCATTCAGATTG-*3′*
MoRdrp3-R	*5′*-GTTAATGTGATGCGACAGTGGG-*3′*

CHAPTER IV

DEEP SEQUENCING ANALYSIS OF SMALL RNA IN *PYRICULARIA ORYZAE*

1. Introduction

New classes of sRNAs other than classical sRNA species, such as siRNA and miRNA, have been found in recent deep sequencing analysis with high-throughput sequencing innovations. One of such sRNA species derived from tRNA, named tRNA-derived small RNA, has attracted broad attention. There are mainly two types of tsRNAs, including tiRNA and tRF, which differ in the cleavage position of the precursor or mature tRNA transcript (Siqi Li, 2018).

tRFs have been defined in several deep sequencing studies (Jöchl et al., 2008; Kawaji et al., 2008; Nunes et al., 2011). tRFs typically come from either the 5’ or 3’ of tRNA genes with lengths between 27 – 40 nt. But 22nt members have also been identified in certain species (Kawaji et al., 2008; Nunes et al., 2011). Biogenesis of tRFs is derived from ribonuclease activity inside or closing the anticodon loop, which creates tRNA-derived small RNAs that correlate to either tRNA halves. It has also been shown that Dicer is responsible for processing tRNA-Gln into 20nt tRFs in length (Cole et al., 2009). An increasing body of evidence indicates that tRFs play a role in growth and reproduction, regardless of how they are made. For example, in the human fungal pathogen *Aspergillus fumigatus,* tRFs have been shown to down-regulate protein synthesis (Jöchl et al., 2008).

In *P. oryzae*, tRFs were relatively more plentiful in appressoria and spores compared to mycelia (Nunes et al., 2011). This is in agreement with the idea that tRFs are involved in controlling protein synthesis downward. Since mycelial tissues are rapidly growing, mature tRNAs molecules are likely required at this developmental stage. Recent evidence in human indicates that tRFs have a complex mechanism of biogenesis that gives rise to different forms of tRFs having dynamic functions in silencing RNA. These tRFs have a group of 5'-phosphate and 3'-hydroxyl and have been divided into two

separate categories. Type I tRFs are processed by means of Dicer from a mature cytoplasm tRNA molecule and are involved in target transcript downregulation in trans. The 3 'end of type II tsRNAs is generated from the termination of RNA polymerase III transcriptions (Haussecker et al., 2010).

2. Materials and methods

2.1. Fungal RNA extraction and quantitative RT-PCR

Total RNA extraction and preparation of cDNA were carried out as previously mentioned (Vu et al., 2013) with a few modifications. Using Sepasol RNA I Super (Nacalai Tesque, Kyoto), the total RNA was isolated from fungal mycelia powder. Total RNA was then applied to cDNA synthesis using ReverTra Ace qPCR RT master mix with genomic DNA remover KIT (Toyobo, Japan). The qRT-PCR assay was performed using GeneAce SYBR qPCR Mix α (Nippon gene, Japan) as directed by the manufacturer with different target primers and an internal control gene (actin). The target mRNA level, relative to the mean of the housekeeping gene of reference, was measured using the comparative Ct procedure.

2.2. Immunoprecipitation, small RNA extraction

Fungal mycelia were ground in liquid nitrogen with mortar and pestle and moved to the lysis buffer [50mM Tris-HCl (pH7.5), 150mM NaCl, 1mM EDTA, and 1% TritonX-100]. After vortex mixing, cell lysate was collected for 3 mins at 4°C by centrifugation at 12,000xg and incubated at 4°C with the agarose gel (Sigma-Aldrich) affinity Anti-FLAG M2 for 3 hours on rotation. After three washes with TBS, FLAG-tagged protein was eluted from the agarose gel affinity by incubating at 4°C for 30 minutes with 150ng/µl FLAG peptide. The eluted supernatant was collected by centrifugation at 8,000xg for 30 seconds at 4°C.

For AGO-associated sRNA sequencing, phenol–chloroform extraction and ethanol precipitation were used to retrieves RNAs from the FLAG-immunoprecipitates. An equivalent amount of phenol: chloroform:isoamyl alcohol solution was added to the FLAG-tagged protein solution, and mixed until it became emulsion. Then the samples was centrifuged for 5 minutes at 4°C at 13,000rpm, and the aqueous phase (upper layer) was moved to a new tube. An equivalent volume of chloroform was added and mixed by inverting the tube. After centrifugation at 13,000rpm for 5 minutes at 4°C, the aqueous phase (upper layer) was transferred to a new tube and 10% volume of 3M CH_3COONa and 2.5 volume of ethanol (99.5%) were added. RNA was recovered by centrifugation at 14,000rpm for 15 minutes after incubation at -20^{o}C for 2 h. After washing with 70% ethanol, RNA was dissolved in nuclease-free water and stored at -80^{o}C.

2.3. High-throughput sequencing

To construct sRNA library for high-throughput sequencing, indexed cDNA libraries were prepared according to the manufacturer's instructions with the NEXTflex Small RNA-Seqv3 package for Illumina (BiooScientif). Using Agencourt AMPure XP beads, the cDNA items were filtered and enriched with PCR to create the final cDNA double-stranded library.

2.4. Northern blots

10µg of total RNA was separated on a ure denaturing 15% polyacrylamide gel, and transferred electrophoretically to a Hybond-N+ Nylon filter membrane. After transfer, the membrane was cross-linked using a UV cross-linker. The membrane was first prehybridized in a hybridization buffer (Ultrahyb buffer, Ambion, Austin, TX, USA) for at least 1h at 42°C, followed

by hybridization with a specific probe overnight. A 22nt fluorescein-labeled oligos complementary to each of 5' terminal sequence of RNA-Glu (CTC) and 3' terminal sequence of tRNA-Gln (CTG) was made and used as a probe. Afterward, the membrane was washed 3 times with 2xSSC containing 0.1% SDS and 1 time of 0.1x SSC/0.1%SDS for 15 minutes at the same temperature.

3. Results

3.1. Components require for biogenesis of tRNA-derived small RNAs

Because a fraction of sRNAs had previously been domonstrated to be methylguanosine-capped in *P. oryzae*, we developed cDNA libraries with TAP-treated sRNAs without gel-based size selection. In addition, adapters with 4 randomized bases at the ligation junctions were used in library construction to eliminate ligation bias. After removal of the adaptor, each sample up 26 to 44 million sRNA reads sized 16 to 38nt were obtained (Table 4-1). The length distributions of sRNAs in WT, rdrp1/2/3, and dcl1/2 were shown in Fig. 4-1a. The number of sRNA in WT was peaked at 19 nt, which corresponds to the size of siRNAs in *P. oryzae* and decreased gradually as the length of sRNA increased with a few slight peaks. The percentage of shorter sRNA (16-20nt) in both rdrp1/2/3 and dcl1/2 was reduced compared to that in WT, and several major peaks were observed at 22, 30, and 33-34nt in rdrp1/2/3, and 29 and 33-34nt in dcl1/2, suggesting that drp1/2/3 and dcl1/2 may have certain limitations in the processing of longer sRNAs.

The read mapping to the *P. oryzae* reference genome (70–15 strain) was performed with a cut-off of 90% coverage and 90% identity. In cDNA libraries, the concentrations of mapped reads were 90.5–95.0% (Table 4-1). The data also show that levels of rRNA-derived sRNAs decreased in both Δrdrp1/2/3 and Δdcl1/2, while levels of tRNA-derived sRNAs increased

significantly. In Δdcl1/2 this phenomenon was more noteworthy. Sequence quantities mapped to specific RNAi targets such as repeats (transposable elements) and mycoviruses (MVs), were also substantially impaired by the absence of the DCL and RDRP genes. sRNAs from TEs and MVs were substantially reduced in Δdcl1/2, while only TE-derived sRNAs were reduced in Δrdrp1/2/3. I analyzed the size distribution of MV-derived sRNAs TE (Figures 4-1b, c) to further answer this question. MV-derived siRNA was much more abundantly observable in Δrdrp1/2/3 than in WT. PoOLV1 to 3 belonging to *Narnaviridae* and their related RNAs were the mycoviruses analyzed in this thesis. Because these viruses are all RNA viruses, intermediate viral replication should have been targeted at RNA silencing and used as substrates of DCL for biogenesis of MV siRNA. Thus, the results indicated that the use of host-encoded RdRP did not intensify MV siRNA. At low rates, without a recognizable peak, MV-derived sRNAs were detectable even in Δdcl1/2. In comparison, a high peak corresponding to siRNA was observed at 19nt in TE-derived sRNAs of WT. Nevertheless, the peak was not observed in either Δdcl1/2 or Δrdrp1/2/3, suggesting that both DCL and RdRP are important for TE-derived siRNA biogenesis.

Fig. 4-2 shows the size distribution of tRNA-derived sRNAs. tsRNAs longer than 27nt were more plentiful with major peaks at 29 and 34nt relative to those in WT in Δrdrp1/2/3 and Δdcl1/2, as opposed to those in WT. The two main peaks related to those observed in total sRNAs of Δdcl1/2 and Δrdrp1/2/3 (Fig. 4-1a). More than half of the 29-30nt tsRNA reads were generated from tRNA-Glu (CTC) consisting of 9 molecular tRNA species in both Δrdrp1/2/3 (51.3%) and Δdcl1/2 (62.0%). These proportions were significantly higher in WT's 29-30nt tsRNA reads than the ratio (38.4%) of tRNA-Glu (CTC). Meanwhile, 55.5% of WT's 33-34nt tsRNA reads were derived from tRNA-Asp (GTC), consisting of 10 molecular tRNA species but its ratio was decreased to 39.1% and 42.6% in Δrdrp1/2/3 and Δdcl1/2,

respectively. This was attributed in part to a rise in reads resulting from tRNA-Glu (CTC) at 33-34nt in both Δrdrp1/2/3 (33.8%) and Δdcl1/2 (27.3%) compared to WT (17.9%). Notably, with shorter (17-19nt) tsRNA sequences, the number of mapped reads decreased on 154 tsRNA species (81.9%) in Δrdrp1/2/3 and 140 tsRNA species (74.5%) in Δdcl1/2 given the overall rise in tsRNAs in the mutants. In comparison, with the 29-30nt tsRNA sequences, only 6 and 9 tsRNA species in Δrdrp1/2/3 and Δdcl1/2, respectively, reported a decline in the number of mapped reads compared to that in WT. These findings discovered that longer tsRNAs are enriched in both Δrdrp1/2/3 and Δdcl1/2 and shorter tsRNAs commonly are depleted. However, each tsRNA species are influenced quite differently by the lack of the RNA silencing components.

To further examine in more detail the effect of the loss of the DCL and RdRP genes on the biogenesis of tRNA-derived sRNAs, we based on two tRNA sequences, tRNA-Glu (CTC) and tRNA-Gln (CTG), from which abundant 5' tRF and 3'tRF species were formed in WT, respectively. Although the amount of shorter 5 'sequences (16 to 27nt in length) was 42.2 % among the 5' terminus tsRNAs in WT, it was 9.3 % and 8.0 % in both Δrdrp1/2/3 and/or Δdcl1/2 (Fig. 4-3a), suggesting that Δrdrp1/2/3 and Δdcl1/2 have a short tsRNA biogenesis deficiency. The highest peak was observed at 35nt in Δrdrp1/2/3. This tsRNA sequence corresponds to 5’ half of tRNA-Glu (CTC), and thus, 5’ tiRNA (Fig. 4-3b). As expected, a strong peak appeared at 29nt in Δdcl1/2. The 3’ terminus of the 29nt sequence was located in the stem structure of the anti-codon loop (Fig. 4-3b). These findings indicate that the absence of RNA components specifically or implicitly facilitates the biogenesis of 5' tiRNAs tRNA-Glu (CTC), or limits their turnover and/or processing to shorter tsRNA.

Only the shortest and the longest tsRNAs have observed significant shifts (Fig. 4-3d). tsRNA of 18 nt, likely major 3’tRF of tRNA-Gln (CTG),

accounted for 26.4% of the CCA-added 3’ tsRNAs in WT but it decreased to 11.8% and 11.4% in Δrdrp1/2/3 and Δdcl1/2, respectively. Directly opposed to this, the percentages of the longest reads likely corresponding to 3'tiRNA of tRNA-Gln (CTG) improved to 31.2% in Δrdrp1/2/3 and 34.6% in Δdcl1/2 compared to those in WT (23.2%).

Notably, during this study, we found that the ratio of CCA added 3' tsRNAs was substantially reduced in Δrdrp1/2/3 (59.3%) and Δdcl1/2 (38.7%) compared to that of WT (75.6%) among reads mapped to 3' half of tRNA-Gln (CTG). Then, 3' ends of tRNA-Gln (CTG) 3' tsRNA is investigated by counting sequences with the same terminus 3' in them. In Δdcl1/2, a large proportion of the 3 'tsRNAs were possibly immature and had their 3' termini in the middle of the acceptor stem. Also included in this group was the most abundant 29nt tsRNA of tRNA-Gln (CTG), which begins from the anticodon stem and ended at the center of the acceptor stem. To know the degree to which DCL and RdRP are implicated in tRNA maturation, we do the same analyzes using all tRNA sequences. Results revealed that 60.8 % of the reads mapped to 3 'half of tRNA had the CCA sequence at the 3 terminus in WT, while the portion was reduced to 45.6 % in Δdcl1/2 terminus. By comparison, the rate of Δrdrp1/2/3 (59.1%) was at a level similar to WT.

Overall, our results indicate that the RdRP and DCL proteins, with a greater influence of the latter, play roles directly or indirectly in the maturation of tRNA, or at least in the rapid elimination of immature tRNA products from the cell.

3.2. Components require for biogenesis of rRNA-derived sRNAs

The proportion of sRNAs (srRNA) derived from rRNA decreased significantly in Δrdrp1/2/3 and Δdcl1/2 (Table 4-1). Fig. 4-4 indicates the number of mapped reads in 4 rRNA species (26S rRNA, 18S rRNA, 5.8S rRNA, and 5S rRNA) at each position. Mapped srRNAs were not spread

uniformly but peaked at various amounts at different positions over the rRNA sequences. In fact, at each terminus, except the 3' terminus of 18S rRNA, mapped reads were very plentiful. The effect of the absence of RdRPs and DCLs was seen more distinctly at peaks. In Δrdrp1/2/3 and Δdcl1/2, the number of mapped reads at a peak was generally reduced, relative to that in WT (Fig. 4-4), with a greater degree in the Δdcl1/2. However, as excepted at the 5' terminus of 26S rRNA and 3' terminus of 5S RNA, the number of mapped reads was much higher in either rrdrp1/2/3 than in WT. Fig. 4-5 exhibits the size distribution of srRNA. In Δrdrp1/2/3 and Δdcl1/2, the proportion of srRNAs smaller than 26nt was significantly decreased relative to WT.

Overall, these findings indicated that DCL and RdRP were not essential for the biogenesis of srRNAs but may partly play a role in the process.

4. Discussion

Small non-protein-coding RNAs have played crucial roles in transcriptional and post-transcriptional gene regulation in eukaryotic organisms, such as miRNA and siRNA, piRNA. Recently, a novel class of sRNAs driven from tRNAs have been discovered in various eukaryotes such as *Giardia lamblia* (Li et al., 2008), *Saccharomyces cerevisiae* (Thompson et al., 2008), Arabidopsis (Hsieh et al., 2009), human (Cole et al., 2009) and *Tetrahymena thermophile* (Pederson, 2010). Studies on the biogenesis mechanisms of tsRNA revealed involvement of different kinds of proteins in the process. Those included RNase III family protein Dicer (Babiarz et al., 2008; Cole et al., 2009), the RNase T2 family protein Rny1p in yeast (2009), RNase A superfamily protein angiogenin (Fu et al., 2009), Argonaute (Prior) family proteins (Haussecker et al., 2010), Piwi family proteins Twi12

(Couvillion et al., 2010), Hiwi2 (Keam et al., 2014), and DNA methyltransferase Dnmt2 in mammals (Schaefer et al., 2010).

In this study, I found that tsRNAs longer than 34 nt were highly accumulated in Δdcl1/2 whereas those less than 27 nt were abundant in WT. Hence DCL proteins could play an important role in processing tsRNA into smaller fragments. In contrast, size distribution of rsRNA is not remarkably changed between Δdcl1/2 and WT except that highly enriched srRNA species were substantially depleted in Δrdrp1/2/3 and Δdcl1/2. In HeLa cells, Cole et al. (2009) found that Dicer cleaved tRNA at the D-loop and formed a 5' fragment of 19 nt. In mouse ES cells, Dicer processed tRNA from the 3' end to produce 3' tsRNAs (Babiarz et al. 2008). However, it is known that tsRNA also could be generated by Dicer independent pathways. One of such enzymes is AGO proteinplaying key roles in the RNA interference pathway by forming a catalytic component with various sRNA.

In *S. pombe*, AGO-associated tRNA fragments were highly accumulated in a mutant of the TRAMP complex, which is responsible for degradation of abberant RNAs. This finding indicated that the TRAMP complex prevents abundant rRNAs and tRNAs from entering the siRNA pathways in the wild-type strain. Interestingly, AGO-associated tRNA fragments of 23 nt in *S. pombe* e was generated independent of Dicer (Buhler et al. 2008).

In human cells, Valen et al. (2011) found that TTSa RNAs, a class of small RNAs mapping to the sense strands of 3′UTRs were highly enriched in the Argonaute-IP libraries with size peak at 22-23nt. These results suggested a connection between AGO loading and mRNA 3′ end processing. This is an interesting finding that need to be further elucidation especially on how AGO selects TTSa RNAs.

Dicer and AGO are well-known main components in the RNA silencing pathway. My studies showed that Dicer protein affects processing tsRNA. Many issues should be addressed in the future; how can DCL or AGO

proteins select tRNA or rRNA, and recognize cleavage sites in the their structures? What exactly is the biogenesis mechanism of sRNA such as tsRNA or rsRNA? Furthermore, what is the biological function of tsRNA and rsRNA?

Tables and figures

Table 4-1. Mapping of sRNA reads to different fractions of the *Pyricularia oryzae* genome

	Total reads	rRNA	tRNA	Exon	Intron	Intergenic	snRNA_snoRNA	Mycovirus	Repeats	Mitochondoria	unmapped
WT	26,207,525	13,256,827	4,311,810	697,929	267,437	949,520	105,314	682,091	842,222	2,610,213	
		50.58%	16.45%	2.66%	1.02%	3.62%	0.40%	2.60%	3.21%	9.96%	9.48%
Δdcl1/2	34,466,526	12,110,414	13,127,507	1,086,587	375,038	1,130,923	133,988	460,381	7,498	4,321,693	
		35.14%	38.09%	3.15%	1.09%	3.28%	0.39%	1.34%	0.02%	12.54%	4.97%
Δrdrp1/2/3	44,388,757	18,859,560	12,569,215	1,426,616	586,583	1,455,667	195,353	1,697,905	7,285	4,395,077	
		42.49%	28.32%	3.21%	1.32%	3.28%	0.44%	3.83%	0.02%	9.90%	7.20%

Table 4-2. RPM of 10 representative such srRNA species

Sequence	WT	dicer	rdrp	ago1	ago2	ago3
TCTTGGATTTATTGAAGACTA	217	42	48	3199	3153	44
GATTTATTGAAGACTA	59	19	22	4309	3441	125
TTGACCCGTTCGGCACCTT	50	0	21	13666	3342	1225
TGACCCGTTCGGCACCTTA	152	20	31	23510	11227	493
CGTTACGATCTGCTGAGGGTA	570	228	604	6192	13645	138
ACGGCGGCGGGGGCCCCGGGCAGAGT	19	12	15	1741	6041	38231
TGGTTTTTGCGGTTGTCCGA	116	56	126	4253	3915	366
TGGATTGTTCACCCACTA	254	107	146	3908	2512	161
TGGTAGGACGCCGAACCTC	1178	373	381	22633	6668	125141
GGTCCGGTGCGCCCTCGACGTCCC	14	11	11	5288	966	8884

Table 4-3. Composition of used medium

Medium name	**Composition**	
PDA (1000mL)	Potato Dextrose Broth	24g
	Agar Powder	15g
LB-amp (1000mL)	Tryptone	10g
	Yeast Extract	5g
	NaCl	10g
	Ampicillin	100µg/mL
CM 5%sucrose (1000mL)	Yeast Extract	3g
	Casamino acids	3g
	Sucrose	5g
CM 20%sucrose (1000mL)	Yeast Extract	3g
	Casamino acids	3g
	Sucrose	200g
50xTAE buffer (1000mL)	Tris	242
	Acetic acids	57mL
	EDTA 2Na(2H20)	18.6g
Agarose gel 0.7% (1000mL)	Agarose Powder	7g
	1XTAE buffer	1000mL
Loading buffer	Glycerol	30%

	Bromophenol blue	0.25%
	Xylene cyanol	0.25%
	30mM EDTA	
Ethidium bromide	Ethidium bromide	500μg/L
	1XTAE buffer	
STC buffer	Sucrose	20%
	Tris-HCl	25mM
	CaCl2	25mM
PEG60%	Polyethylene glycol	60%
	Tris-HCl	25mM
	CaCl2	25mM
TE buffer	Tris-HCl	10mM
	EDTA	1mM

a

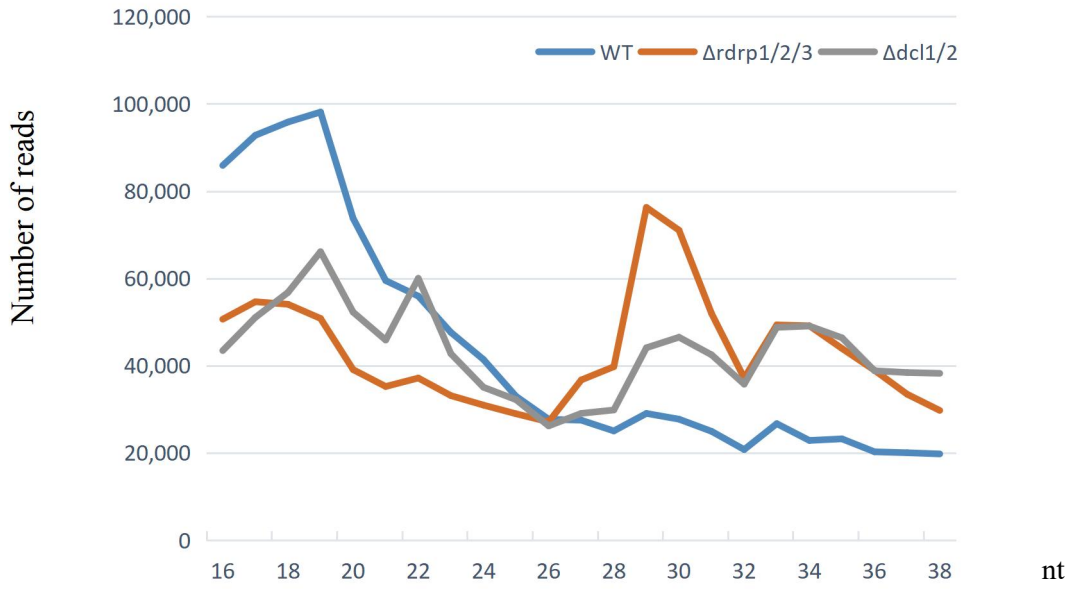
120,000
100,000
80,000
60,000
40,000
20,000
0
Number of reads
WT
Δrdrp1/2/3
Δdcl1/2
16
18
20
22
24
26
28
30
32
34
36
38
nt

b

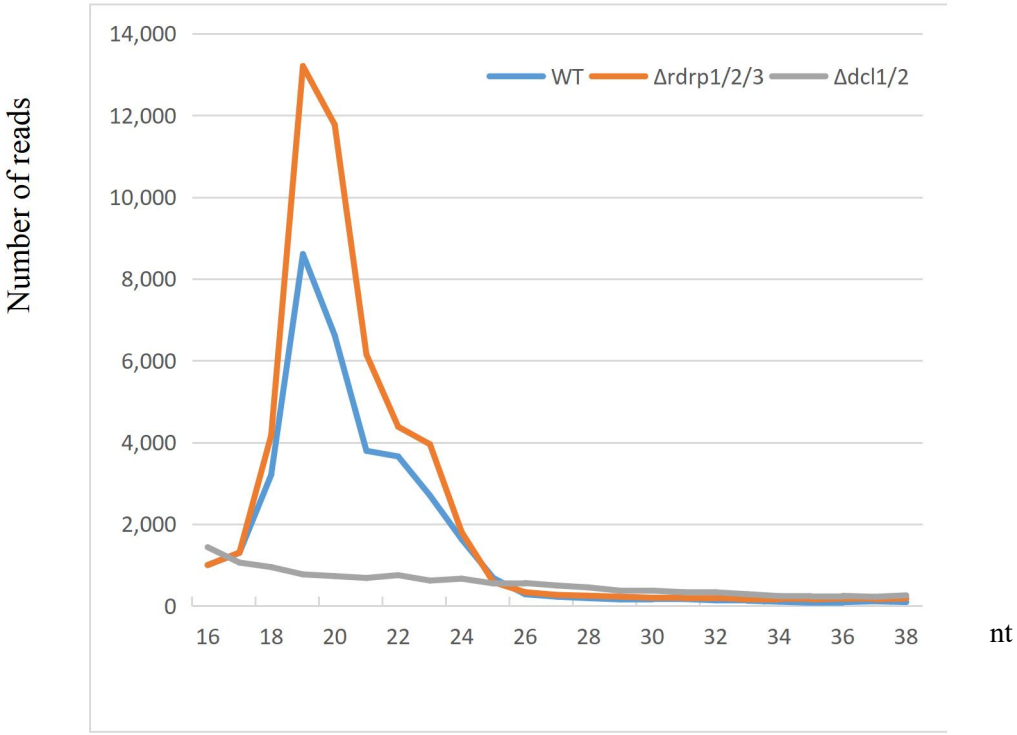
14,000
12,000
10,000
8,000
6,000
4,000
2,000
0
Number of reads
WT
Δrdrp1/2/3
Δdcl1/2
16
18
20
22
24
26
28
30
32
34
36
38
nt

c

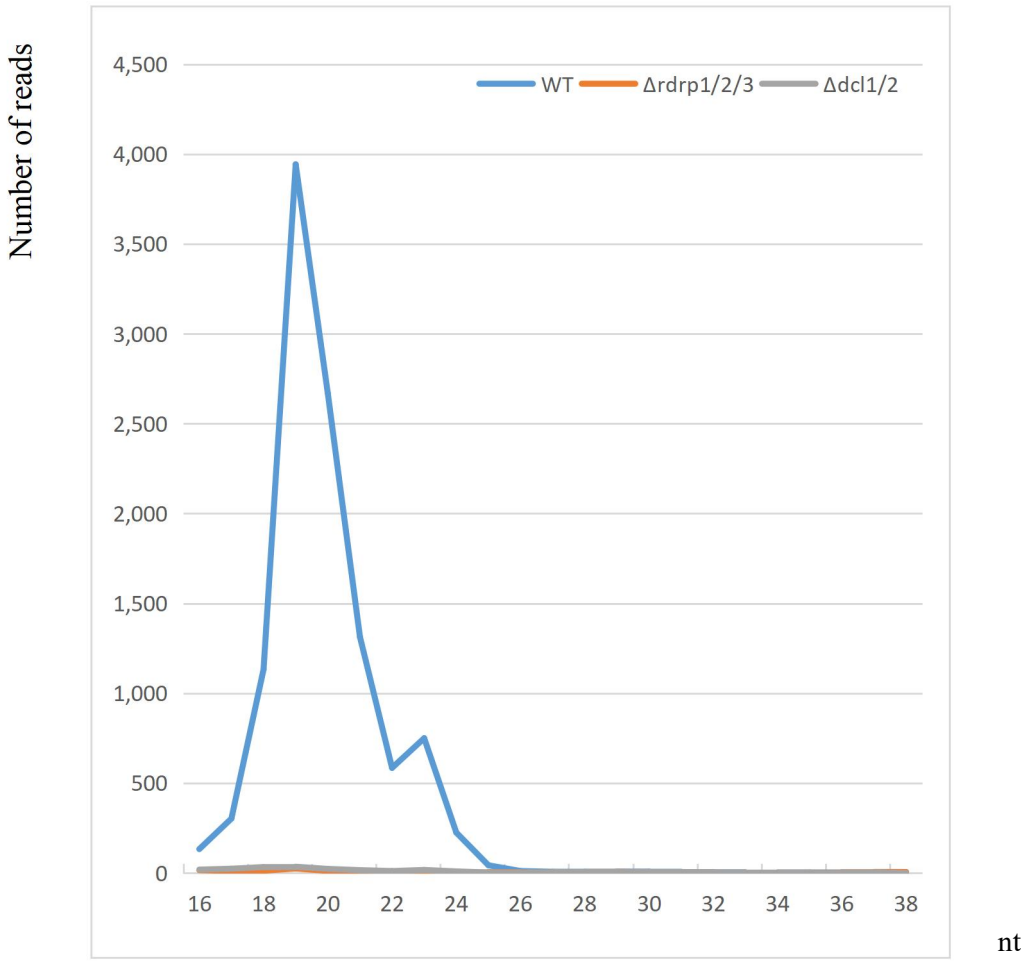

Figure 4-1. The size distribution of sRNAs in WT, Δrdrp1/2/3 and Δdcl1/2.

90% of tRNA-Glu (CTC) derived sRNAs were mapped to its 5' half in either WT, Δrdrp1/2/3, or Δdcl1/2. Sequences starting from the 5' terminus of tRNA-Glu (CTC) were extracted and the number of sequences sharing the same 3' terminus was counted. tRNA-Gln (CTG) derived sRNAs were mapped to its 3' half in either WT, Δrdrp1/2/3, or Δdcl1/2. During tRNA maturation, the CCA sequence is added onto the 3' end of tRNA precursors.sequences possessing CCA at the 3' terminus were selected, and the number of sequences sharing the same 5' terminus was counted. **(a)**. The size distribution of sRNAs in WT, Δrdrp1/2/3 and Δdcl1/2. **(b).** The size distribution of MV-derived sRNAs. **(c)**. The size distribution of TE-derived sRNAs

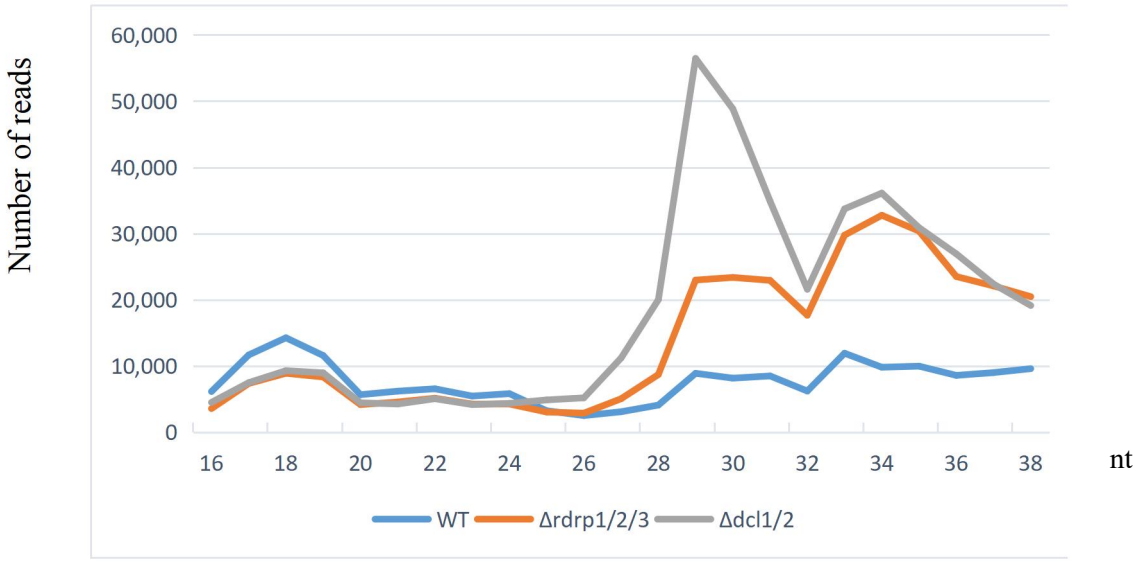

Figure 4-2. The size distribution of tRNA-derived sRNAs. cDNA libraries was developed with TAP-treated sRNAs without gel-based size selection. Adapters with 4 randomized bases at the ligation junctions were used in library construction to eliminate ligation bias. After removal of the adaptor, each sample up 26 to 44 million sRNA reads sized 16 to 38nt were obtained. tsRNAs longer than 27nt were more plentiful with major peaks at 29 and 34nt relative to those in WT in Δrdrp1/2/3 and Δdcl1/2, as opposed to those in WT.

a

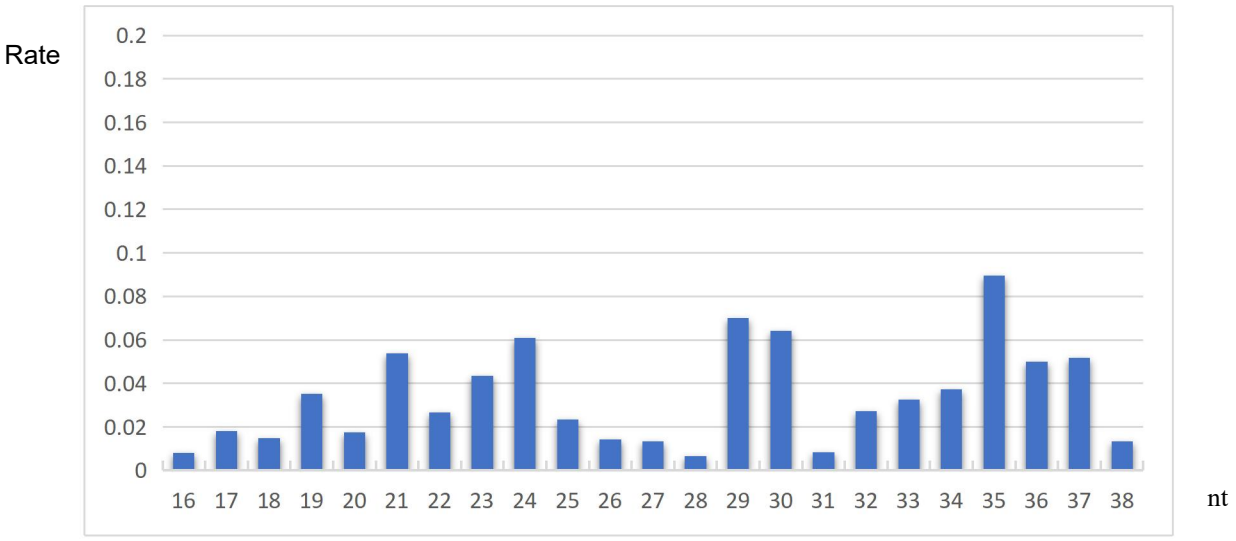
Rate
0.2
0.18
0.16
0.14
0.12
0.1
0.08
0.06
0.04
0.02
0
16 17 18 19 20 21 22 23 24 25 26 27 28 29 30 31 32 33 34 35 36 37 38
nt

b

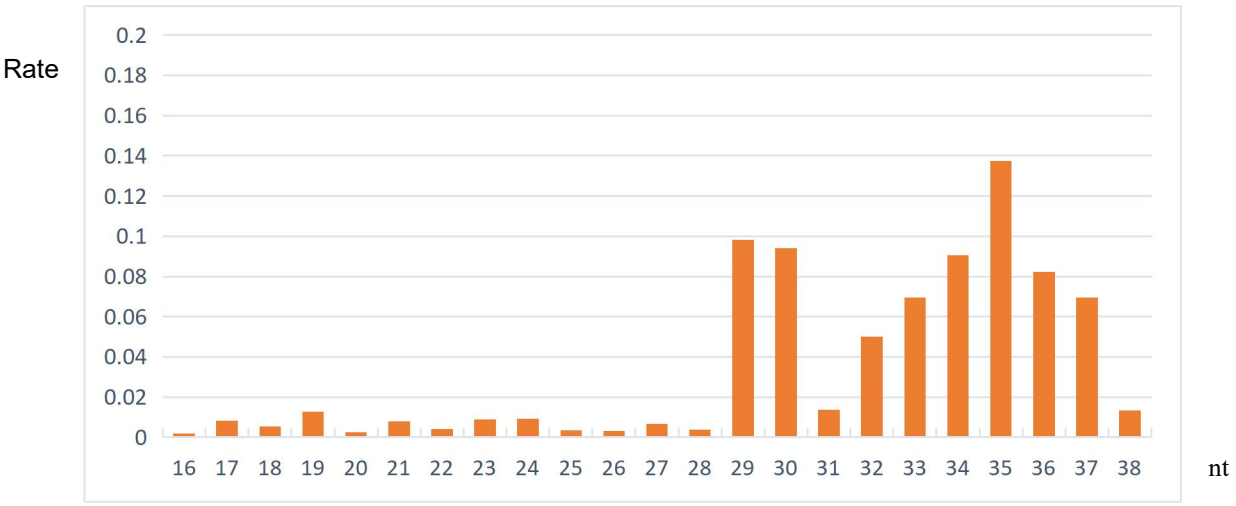
Rate
0.2
0.18
0.16
0.14
0.12
0.1
0.08
0.06
0.04
0.02
0
16 17 18 19 20 21 22 23 24 25 26 27 28 29 30 31 32 33 34 35 36 37 38
nt

c

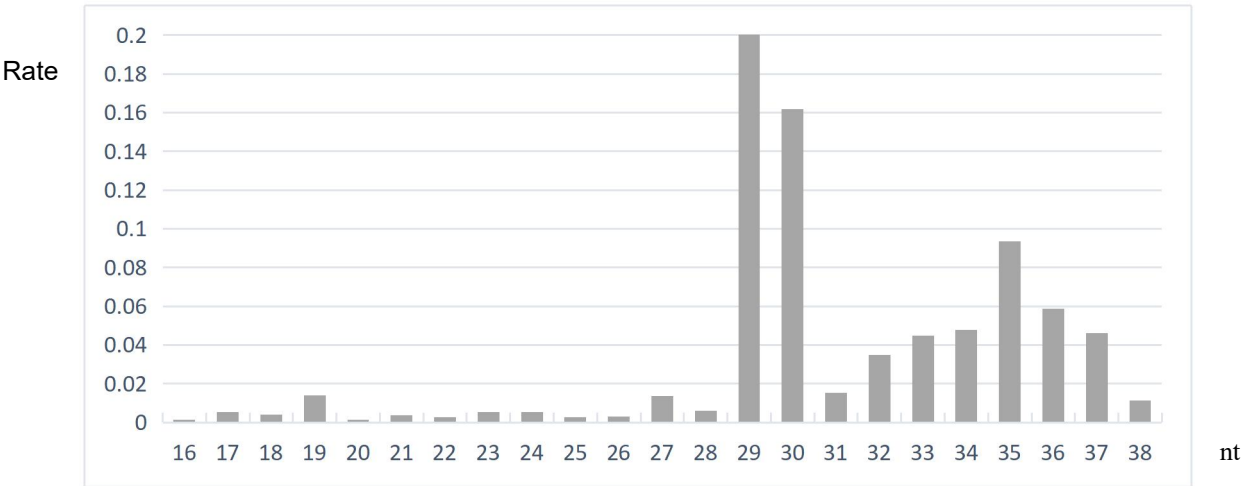
Rate
0.2
0.18
0.16
0.14
0.12
0.1
0.08
0.06
0.04
0.02
0
16 17 18 19 20 21 22 23 24 25 26 27 28 29 30 31 32 33 34 35 36 37 38
nt

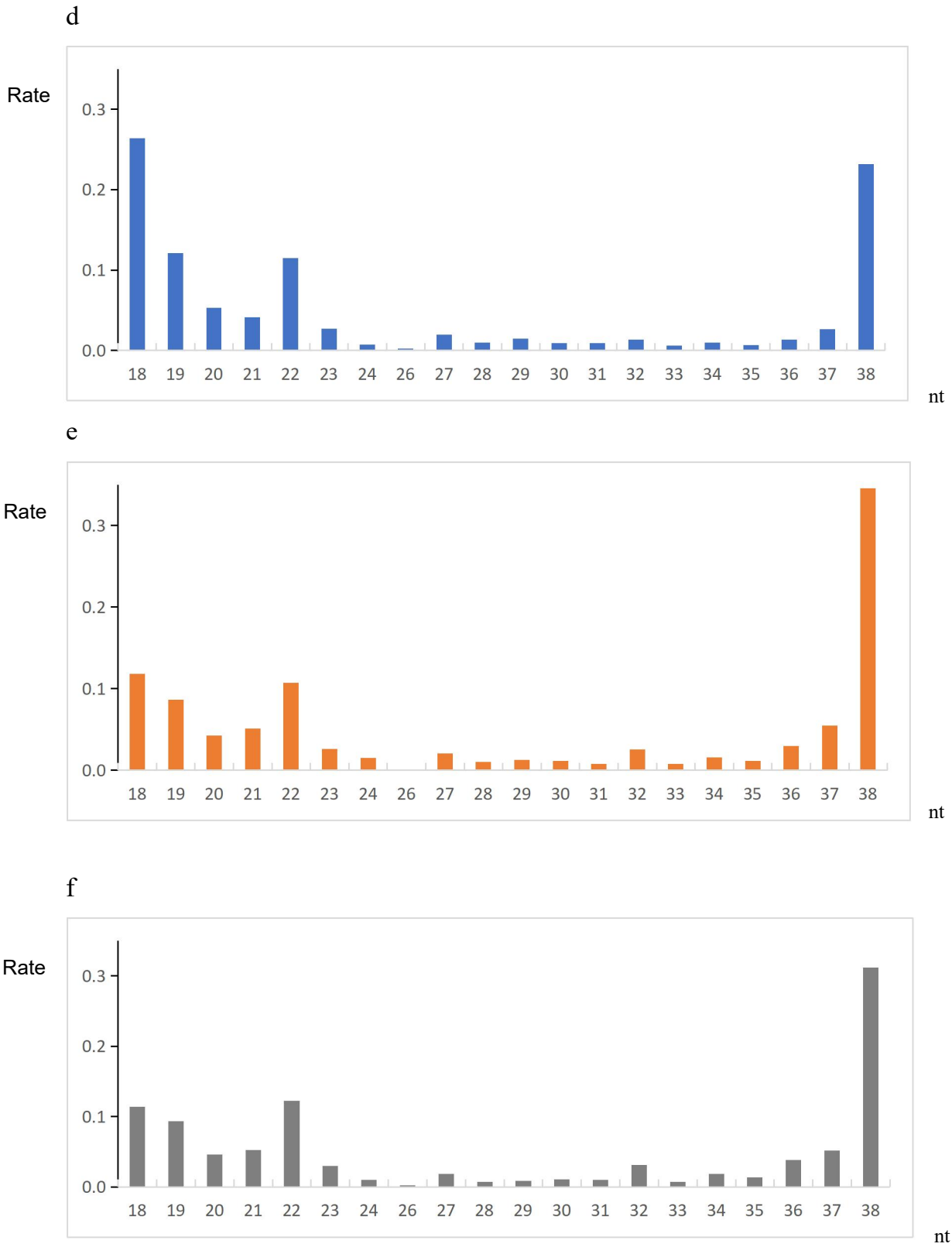

Figure 4-3. The effect of the loss of the DCL and RdRP genes on the biogenesis of tRNA-derived sRNAs. Rate of tRNA-Glu (CTC) and derived sRNAs in WT (blue bar) (a), (d), Δrdrp1/2/3 (orange bar) (b), (e) and Δdcl1/2 (grey bar) (c), (f).

a

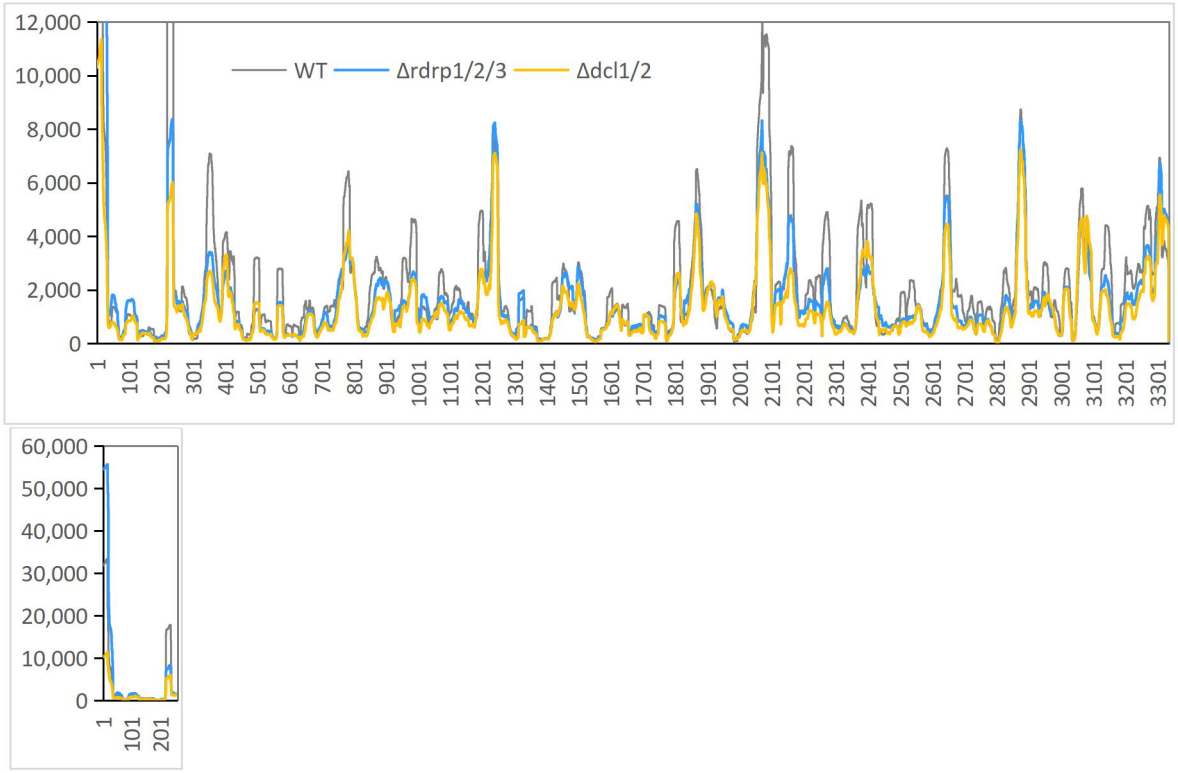

b

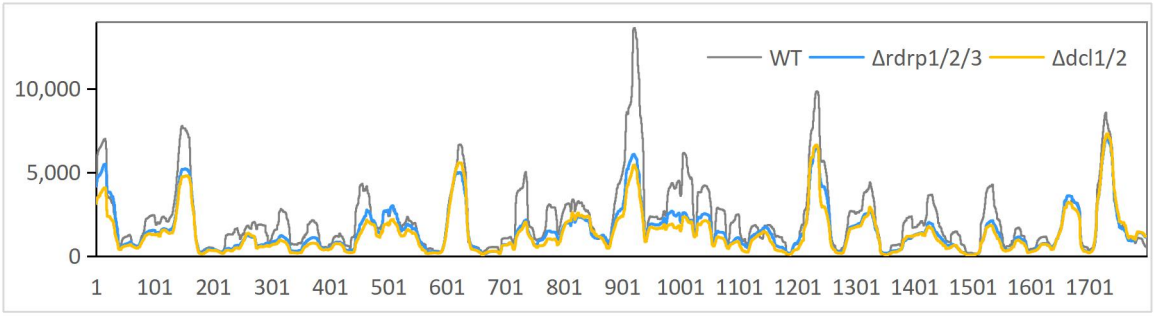

c

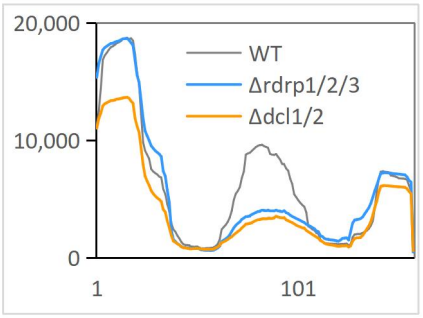

d

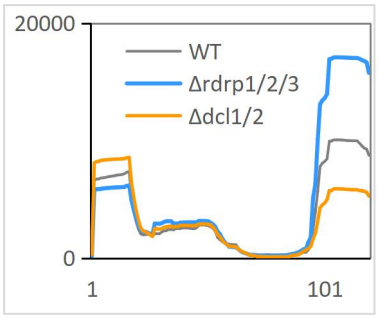

Figure 4-4. The number of mapped reads at every position in 4 rRNA species (a) 26S rRNA, (b)18S rRNA, (c) 5.8S rRNA , (d) 5S rRNA). Reads mapped of WT (gray line), Δdcl1/2 (blue line), Δrdrp1/2/3 (orange line). The effect of the absence of RdRPs and DCLs was seen more distinctly at peaks. In Δrdrp1/2/3 and Δdcl1/2, the number of mapped reads at a peak was generally reduced, relative to that in WT.

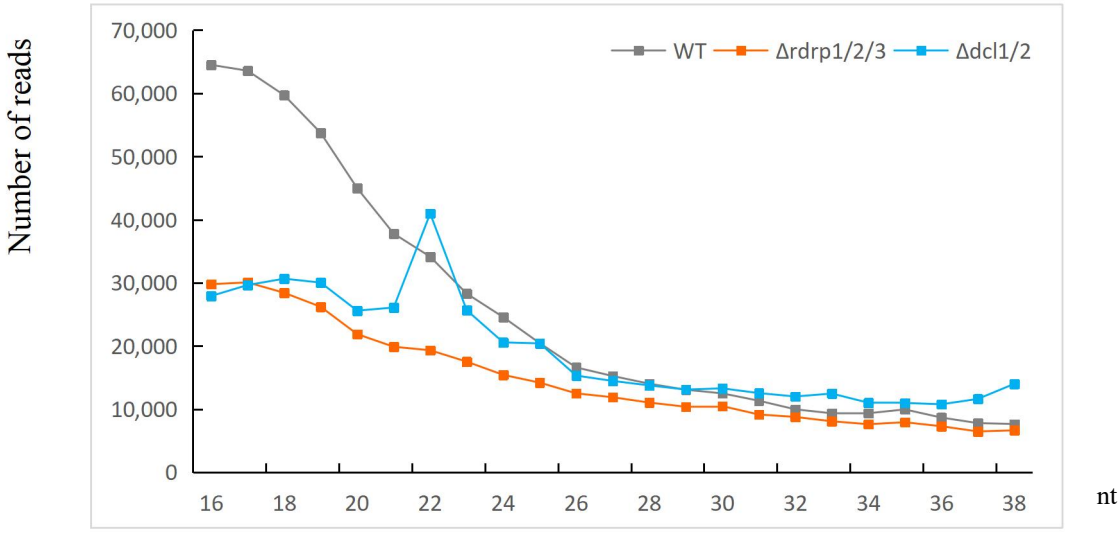

Figure 4-5. The size distribution of srRNAs. Reads mapped of WT (gray line), Δdcl1/2 (blue line), Δrdrp1/2/3 (orange line). In Δrdrp1/2/3 and Δdcl1/2, the proportion of srRNAs smaller than 26nt was significantly decreased relative to WT.

a

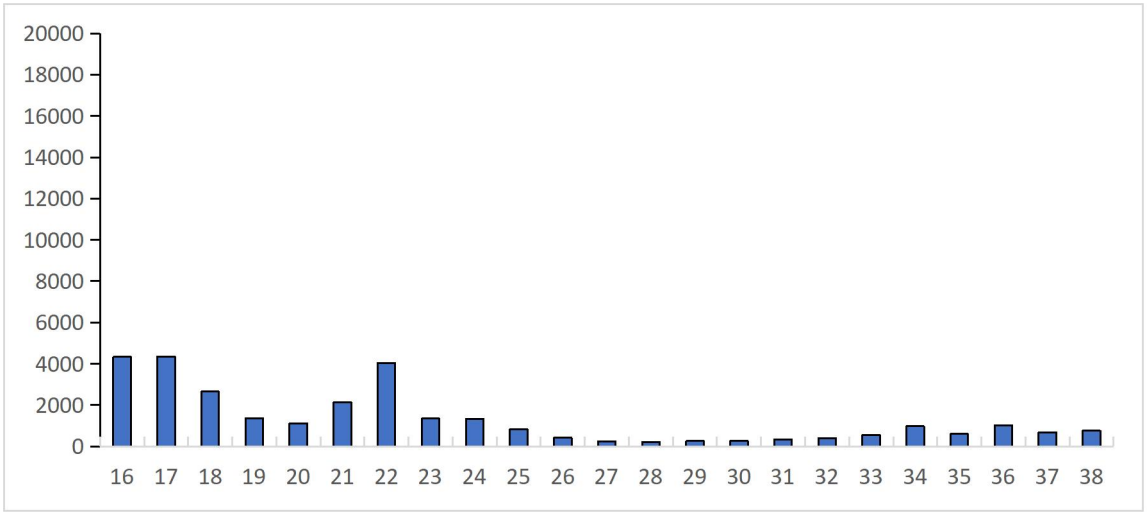

b

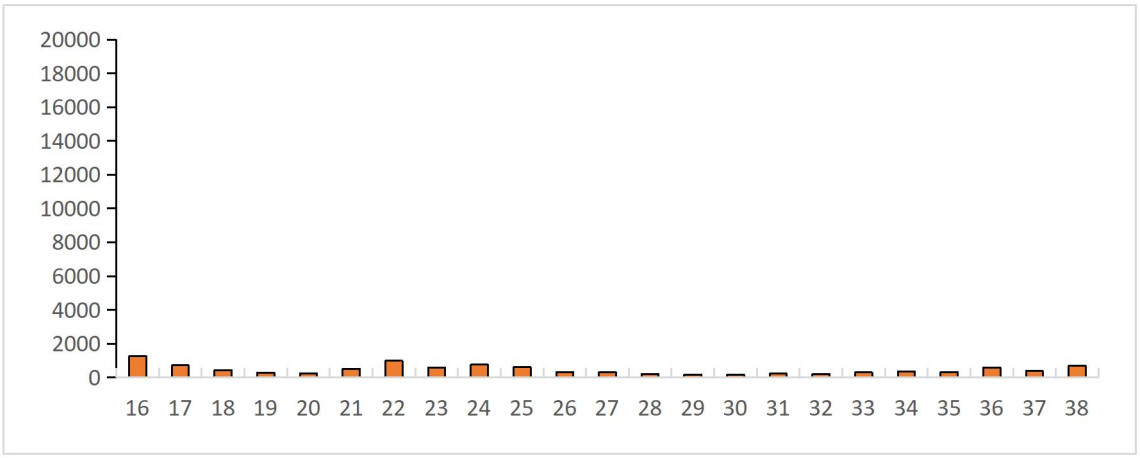

c

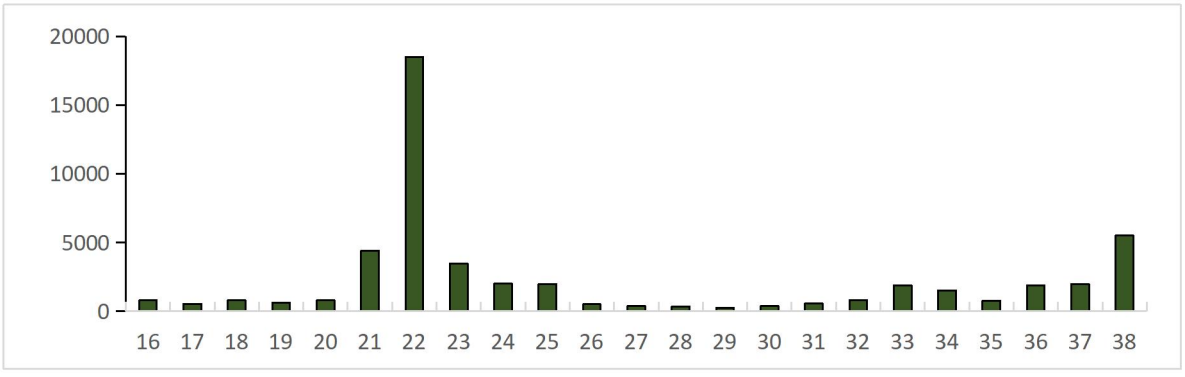

Figure 4-6. The size distribution of sRNAs sharing the 5' terminus of 26S rRNA in WT, Δdcl1/2 and Δrdrp1/2/3. Reads mapped of WT (blue bar) (a), Δdcl1/2 (orange bar) (b) and Δrdrp1/2/3 (dark green bar) (c). The number of mapped reads was much higher in either rrdrp1/2/3 than in WT at the 5' terminus of 26S rRNA.

Acknowledgments

There are various individuals without whom this dissertation probably won't have been composed. First, I would like to express my gratitude to Professor Hitoshi Nakayashiki for providing precious guidance for the duration of this study. Thank you for always being there once I wished for help. I am very much thankful to Professor Katsuhiko Sakamoto and Associate Professor Kenichi Morigaki, for giving me insightful comments and advice. Also, I express my thanks to Dr. Kenichi Ikeda and all my labmates, especially Yusaku Tsukahara and Dang An Thach, for their aides in my own life and exploration during the time we have cooperated at the Laboratory of Cell Function and Structure, Faculty of Agriculture, Kobe University. I am additionally appreciative to all understudies at Laboratory of Plant Pathology, Faculty of Agriculture, and all instructors and staff at Student Affairs Section, Kobe University for their genuine graciousness and companionships during my stay in Japan. I would like to deliver my authentic gratitude to my chief Dr. Vu Thi Bich Hau as well as my kind friends for their countless supports and encouragement. At last, thank my family, who give me their love, support, and encouragement during my studies in Japan.

Kobe, 2023

Dang Ngoc Minh

References

Alberola M, 1996. Molecular structure of a gypsy element of *Drosophila subobscura (gypsyDs)* constituting a degenerate form of insect retroviruses. Nucleic Acids Res. 24:914-923.

Alex E, Natalie D, Chris G, Marte B and Deepa N, 2007. Introduction Epigenetics. Nature. 447: 395.

Almeida R, Allshire RC, 2005. RNA silencing and genome regulation. Trends Cell Biol. 15: 251–258.

Annalisa M, Tiziana A, Giusi R, Rosaria L, Antonio P, Silvia B, Candida Z, Federica B, Ian B, Brittany A, 2014. Targeted DNA methylation by homology-directed repair in mammalian cells. Transcription reshapes methylation on the repaired gene. Nucleic Acids Res. 42(2): 804-821.

Antequera F, Tamame M, Villanueva JR, Santos T, 1984. DNA methylation in the fungi. J. Biol. Chem. 259: 8033–8036.

Asha S, Soniya V, 2017. The sRNAome mining revealed existence of unique signature small RNAs derived from 5.8SrRNA from *Piper nigrum* and other plant lineages. Sci. Rep. 7: 41052.

Banks J, Masson P. and Fedoroff N, 1988. Molecular mechanisms in the developmental regulation of the maize suppressor-mutator transposable element. Genes Dev. 2:1364–1380.

Barkan A, Martienssen RA, 1991. Inactivation of maize transposon Mu suppresses a mutant phenotype by activating an outward-reading promoter near the end of Mu1. PNAS. 88:3502–3506.

Berger SL, Kouzarides T, Shiekhattar R, Shilatifard A, 2009. An operational definition of epigenetics. Genes & Development. 23 (7): 781–3.

Bird A, 2002. DNA methylation patterns and epigenetic memory. Genes Dev. 16(1):6-21.

Black JC, Van Rechem C, Whetstine R, 2012. Histone lysine methylation dynamics: establishment, regulation, and biological impact. Mol Cell. Nov 30;48(4):491-507.

Bond M and Baulcombe C, 2015. Epigenetic transitions leading to heritable, RNA-mediated de novo silencing in *Arabidopsis thaliana*. Proc. Natl. Acad. Sci. USA. 112: 917-922.

Borges F, and Martienssen A, 2015. The expanding world of small RNAs in plants. Nat. Rev. Mol. Cell Biol. 16: 727-741.

Braman J, 2010. In Vitro Mutagenesis Protocols, Third Edition, Humana Press.

Burroughs M et al., 2011. Deep-sequencing of human Argonaute-associated small RNAs provides insight into miRNA sorting and reveals Argonaute association with RNA fragments of diverse origin. RNA Biol.8:158–177.

Cambareri B, Jensen C, Schabtach E, Selker EU, 1989. Repeat-induced G-C to A-T mutations in Neurospora. Science. 244(4912):1571-1575.

Castel E, Martienssen A, 2013. RNA interference in the nucleus: roles for small RNAs in transcription, epigenetics and beyond. Nat. Rev. Genet14:100–112.

Cerutti H, Casas-Mollano A, 2006. On the origin and functions of RNA-mediated silencing: from protists to man. Curr. Genet. 50:81–99.

Chandler V, Walbot V, 1986. DNA modification of a maize transposable element correlates with loss of activity. Proc. Natl Acad. Sci. USA. 83: 1767–1771.

Chandler V, February 2007. Paramutation: from maize to mice. Cell. 128 (4): 641–5.

Chen X, 2009. Small RNAs and their roles in plant development. Annu. Rev. Cell Dev. Biol. 25:21–44.

Chiang P, Gordon R, Tal J, Zeng G, Doctor B, Pardhasaradhi K, McCann P, 1996. S-Adenosyl methionine and methylation. FASEB J. 10 (4): 471–80.

Chomet P, Wessler S, Dellaporta S, 1987. Inactivation of the maize transposable element Activator (Ac) is associated with DNA modification. EMBO J.6: 295–302.

Clare J, Farabaugh P. 1985. Nucleotide sequence of a yeast Ty element: evidence for an unusual mechanism of gene expression. PNAS. 82(9):2829-2833.

Cornellia G, Glenn M, Mark W, Pastan I, Howard B, 1982. The *Rous sarcoma* virus long terminal repeat is a strong promoter when introduced into a variety of eukaryotic cells by DNA-mediated transfection. PNAS. 79: 6777-6781.

Cosgrove S, Boeke D, Wolberger C, 2004. Regulated Nucleosome Mobility and the Histone Code. Nature Structural Molecular Biology. 11: 1037-1043.

Couch C, Kohn M, 2002. A multilocus gene genealogy concordant with host preference indicates segregation of a new species, *Magnaportheoryzae*, from *M. grisea*. Mycologia. 94:683–693.

Cox M, Nelson DR, Lehninger AL. 2005. Lehninger Principles of Biochemistry. San Francisco: W.H. Freeman.

Cremer T, Cremer M, 2010. Chromosome Territories. Cold Spring Harbor Perspectives in Biology. 2 (3): a003889–a003889.

Danuta J, Robert M, Marco G, Ricarda G, David G, Helena A, Taiping C, En L, Jelena T, Magnus L, 2017. DNA methylation of intragenicCpG islands depends on their transcriptional activity during differentiation and disease. PNAS. 114: E7526-E7535.

Dean A, Talbot J, Ebbole J, Farman L, Mitchell K, Orbach J, Thon M, Kulkarni R, Xu R, 2005. The genome sequence of the rice blast fungus *Magnaporthegrisea*. Nature. 434:980–986.

Dorner J, and Coffin J, 1986. Determinants for receptor interaction and cell killing on the avian retrovirus glycoprotein gp85. Cell. 45: 365–374.

Dorner J, and Coffin J, 1985. Molecular basis of host range variation in avian retroviruses. J. Virol. 53: 32–39.

Dupont C, Armant R, Brenner A, 2009. Epigenetics: definition, mechanisms and clinical perspective . Seminars in Reproductive Medicine. 27 (5): 351–357.

Ehrlich M, Gama M, Huang H, Midgett M, Kuo C, McCune A, Gehrke C, 1982. Amount and distribution of 5-methylcytosine in human DNA from different types of tissues or cells. Nucleic Acids Research. 10: 2709–2721.

Fang X and Qi Y, 2016. RNAi in Plants: An Argonaute-Centered View. Plant Cell. 28: 272-285.

Farman L, Tosa Y, Nitta N, Leong S, 1996. MAGGY, a retrotransposon in the genome of the rice blast fungus *Magnaporthe grisea*. Mol. Gen. Genet. 251: 665–674.

Fraser J, Williamson I, Bickmore A, Dostie J, 2015. An overview of genome organization and how we got there: From FISH to Hi-C. Microbiol. Mol. Biol. Rev. 79(3): 347–372.

Fraser P, Bickmore W, 2007. Nuclear organization of the genome and the potential for gene regulation. Nature. 447:413–7.

Freitag M, Lee DW, Kothe GO, Pratt RJ, Aramayo R, Selker EU, 2004. DNA Methylation Is Independent of RNA Interference in *Neurospora*. Science. 304 (5679):1939.

Fu J, Hettler E, Wickes BL, 2005. Split marker transformation increases homologous integration frequency in *Cryptococcus neoformans*. Fungal Genet Biol. 43: 200–212.

Gowda M, Venu C, Raghupathy B, Nobuta K, Li H, Wing R, Stahlberg E, Couglan S, Haudenschild D, Dean R, 2006. Deep and comparative analysis of the mycelium and appressorium transcriptomes of *Magnaporthe grisea* using MPSS, RL-SAGE, and oligoarray methods. BMC Genomics. **7**: 310.

Goyon C, Faugeron G. 1989. Targeted transformation of Ascobolus immersus and de novo methylation of the resulting duplicated DNA sequences. Mol Cell Biol. 9(7):2818-27

Grewal I, 2010. RNAi-dependent formation of heterochromatin and its diverse functions. Curr. Opin. Genet. Dev. 20:134–141

Heng Z, Guohua W, Jiang Q, 2016. Transcription factors as readers and effectors of DNA methylation. Nat Rev Genet. 17(9):551-655.

Hirochika H, Okamoto H, and Kakutani T, 2000. Silencing of retrotransposons in *Arabidopsis* and reactivation by the ddm1 mutation. Plant Cell.12: 357–369.

Hock J, Meister G, 2008. The Argonaute protein family. Genome Biol. 9: 210.

Hopp P, Prickett S, Price L, Libby T, March J, Paul J. 1988. A Short Polypeptide Marker Sequence Useful for Recombinant Protein Identification and Purification. Bio/Technology. 6 (10): 1204–10.

Haussecker D, Yong H, Ashley L, Poornima P, Andrew F, Mark K, 2010. Human tRNA-derived small RNAs in the global regulation of RNA silencing. RNA. Apr;16(4):673-95.

Hua C, Zhao H, Guo S, 2018. Trans-Kingdom RNA Trans-Kingdom RNA Silencing in Plant-Fungal Pathogen Interactions. *Mol. Plant* 11, 235–244, https://doi.org/10.1016/j.molp.2017.12.001.

Ikeda K, Nakayashiki H, Takagi M, Tosa Y, Mayama S, 2001. Heat shock, copper sulfate and oxidative stress activate the retrotransposon MAGGY resident in the plant pathogenic fungus Magnaporthe grisea. Mol Genet Genomics. 266(2):318-325.

Jahner D, Jaenisch R, 1985. Retrovirus-induced de novo methylation of flanking host sequences correlates with gene inactivity. Nature. 315:594–597.

Jain R, Iglesias N, Moazed D, 2016. Distinct Functions of Argonaute Slicer in siRNA Maturation and Heterochromatin Formation.Mol Cell. 63(2):191-205.

Jayaprakash, D, Jabado O, Brown D, Sachidanandam R, 2011. Identification and remediation of biases in the activity of RNA ligases in small-RNA deep sequencing. Nucleic Acids Res. 39: e141.

Jeseničnik T, Štajner N, Radišek S, *et al.*, 2019. RNA interference core components identified and characterised in *Verticillium nonalfalfae*, a vascular wilt pathogenic plant fungi of hops. *Sci Rep* **9**, 8651.

Jenuwein T, Allis D, 2001. Translating the histone code. Science, 293, 1074-1080.

Kadotani N, Nakayashiki H, Tosa Y, Mayama S, 2003. RNA silencing in the phytopathogenic fungus *Magnaporthe oryzae*. Mol Plant Microbe Interact. 16: 769-775.

Kapitonov V, Jerzy J, 2008. A universal classification of eukaryotic transposable elements implemented in Repbase. Nature Reviews Genetics. 9 (5): 411–2.

Kato H, Yamamoto M, Yamaguchi-Ozaki T, Kadouchi H, Iwamoto Y, Nakayashiki H, Tosa Y, Mayama S, Mori N, 2000. Pathogenicity, mating ability and DNA restriction fragment length polymorphisms of *Pyricularia* populations isolated from *Gramineae, Bambusideae* and *Zingiberaceae* plants. J. Gen. Plant Pathol. 66:30–47.

Kim N, Han J, Siomi C, 2009. Biogenesis of small RNAs in animals. Nat. Rev. Mol. Cell Biol. 10:126–139.

Kim A, Terzian C, Santamaria P, et al., 1994. Retroviruses in invertebrates: the gypsy retrotransposon is apparently an infectious retrovirus of *Drosophila melanogaster*. PNAS. 91: 1285–1289.

Lee C, Li L, Gu W, Xue Z, Crosthwaite K, Pertsemlidis A, et al., 2010. Diverse pathways generate microRNA-like RNAs and Dicer-independent small interfering RNAs in fungi. Mol. Cell. 38: 803-814.

Lee S, Shibata Y, Malhotra A, Dutta A, 2009. A novel class of small RNAs: tRNA-derived RNA fragments (tRFs). Genes Dev. 23: 2639-2649.

Li E, Beard C, Jaenisch R, 1993. Role for DNA methylation in genomic imprinting. Nature. 366: 362–365.

Li W, Zhang P, Fellers JP, Friebe B, Gill BS, 2004. Sequence composition, organization, and evolution of the core *Triticeae* genome. Plant J. 40: 500–11.

Li L, Chang S, Liu Y, 2010. RNA interference pathways in filamentous fungi. Cell Mol. Life Sci. 67: 3849-3863.

Lippman Z, Gendrel AV, Black M, Vaughn MW, Dedhia N, McCombie WR, Lavine K, Mittal V, May B, Kasschau KD, et al., 2004. Role of transposable elements in heterochromatin and epigenetic control. Nature. 430:471–476.

Lisa M, Thuc L, Guoping F, 2012. DNA Methylation and Its Basic Function. Neuropsychopharmacology.38: 23–38.

Lister R, O'Malley RC, Tonti-Filippini J, Gregory D, Berry C, Millar AH, Ecker R, 2008. Highly integrated single-base resolution maps of the epigenome in Arabidopsis. Cell. 133:523–536.

Macleod D, Charlton J, Mullins J, Bird A, 1994. Sp1 sites in the mouse aprt gene promoter are required to prevent methylation of the CpG islands. Genes Dev.8: 2282–2292.

Mallory C, Hinze A, Tucker R, Bouche N, Gasciolli V, Elmayan T, Lauressergues D, Jauvion V, Vaucheret H, Laux T, 2009. Redundant and specific roles of the ARGONAUTE proteins AGO1 and ZLL in development and small RNA-directed gene silencing. PLoS Genet. 5: e1000646.

Marjori M, Rebecca M, 2014. RNA-directed DNA methylation: an epigenetic pathway of increasing complexity Nature Reviews Genetics. 15: 394–408.

Matzke M, Kanno T, Huettel B, Daxinger L, Matzke AJ, 2006. RNA-directed DNA methylation and Pol IVb in Arabidopsis. Cold Spring Harb Symp Quant Biol. 71:449-59.

Matzke M, Mette MF, Jakowitsch J, Kanno T, Moscone EA, van der Winden J, et al., 2001. A test for transvection in plants: DNA pairing may lead to trans-activation or silencing of complex heteroalleles in tobacco. Genetics.158:451–461.

Matzke A, Aufsatz W, Kanno T, Mette M, Matzke J, 2002. Homology-dependent gene silencing and host defense in plants. Adv Genet. 46: 235-75.

McClintock B. June 1950. The origin and behavior of mutable loci in maize. PNAS. 36 (6): 344–55.

McHale T, Roberts I, Noble S, et al., 1992. *Cf*T-I: an LTR-retrotransposon in *Cladosporiumfulvum*, a fungal pathogen of tomato. Mol. Gen. Genet. 233: 337–347.

Meng X, Bin Y, 2015. siRNA-directed DNA Methylation in Plants.Curr Genomics. 16(1): 23–31.

Mette F, Aufsatz W, van der Winden J, Matzke A, Matzke J, 2000. Transcriptional silencing and promoter methylation triggered by double-stranded RNA. EMBO J. 19: 5194-5201.

Moazed, D, 2009. Small RNAs in transcriptional gene silencing and genome defence. Nature. 457: 413-420.

Mochama P, Jadhav P, Neupane A, Marzano L, 2018. Mycoviruses as triggers and targets of RNA silencing in white mold fungus Sclerotinia sclerotiorum. Viruses. 10:214. doi: 10.3390/v10040214.

Murata N, Aoki T, Kusaba M, Tosa Y, Chuma I, 2014. Various species of Pyricularia constitute a robust clade distinct from *Magnaporthe salvinii* and its relatives in Magnaporthaceae. J. Gen. Plant Pathol. 80: 66–72.

Nakayashiki H, 2005. RNA silencing in fungi: mechanisms and applications. FEBS Lett. 579: 5950-5957.

Nakayashiki H, Matsuo H, Chuma I, Ikeda K, Betsuyaku S, Kusaba M, Tosa Y, Mayama S, 2001. Pyret, a Ty3/Gypsy retrotransposon in *Magnaporthe grisea* contains an extra domain between the nucleocapsid and protease domains. Nucleic Acids Res. 29 (20): 4106-4113.

Nakayashiki H, Kiyotomi K, Tosa Y, Mayama S, 1999. Transposition of the retrotransposon MAGGY in heterologous species of filamentous fungi. Genetics. 153: 693–703.

Neupane A, Feng C, Mochama K, Saleem H, Lee Y, 2019. Roles of Argonautes and Dicers on Sclerotinia sclerotiorum Antiviral RNA Silencing. Front. Plant Sci. 10:976. doi: 10.3389/fpls.2019.00976.

Neuvéglise C, Feldmann H, Bon E, Gaillardin C, Casaregola S, 2002. Genomic evolution of the long terminal repeat retrotransposons in hemiascomycetous yeasts. Genome Res. 12(6):930-43.

Nunes C, Gowda M, Sailsbery J, Xue M, Chen F, Brown E, Oh Y, Mitchell K, Dean A, 2011. Diverse and tissue-enriched small RNAs in the plant pathogenic fungus, *Magnaporthe oryzae*. BMC Genomics. 12: 288.

Parker R, Sheth U, 2007. P bodies and the control of mRNA translation and degradation. Mol Cell. 25: 635-646.

Pham K, Inoue Y, Vu B, Nguyen H, Nakayashiki H, 2015. Correction: MoSET1 (Histone H3K4 Methyltransferase in *Magnaportheoryzae*) Regulates Global Gene Expression during Infection-Related Morphogenesis. PLOS Genetics. 11(12): e1005752.

Phillips T, 2008. The role of methylation in gene expression. Nature Education 1, 116.

Phillips T, 2008. Small non-coding RNA and gene expression. Nature Education 1(1):115.

Pray L, Zhaurova K, 2008. Barbara McClintock and the discovery of jumping genes (transposons). Nature Education 1(1):169.

Qutob D, Chapman P, Gijzen M, 2013. Transgenerational gene silencing causes gain of virulence in a plant pathogen. *Nature commun.* **4**, 1349–1349, https://doi.org/10.1038/ncomms2354.

Keith S, Martienssen R, 2007. Transposable elements and the epigenetic regulation of the genome.Nature Reviews Genetics.8:272-285.

Raman V, Simon S, Demirci F, Nakano M, Meyers B, Donofrio M, 2017. Small RNA functions are required for growth and development of magnaporthe oryzae. Mol. Plant-Microbe Interact. 30:517–530. doi: 10.1094/MPMI-11-16-0236-R.

Reik W, 2007. Stability and flexibility of epigenetic gene regulation in mammalian development. Nature. 447 (7143): 425–32.

Saigo K, Kugimiya W, Matsuo Y, et al., 1984. Identification of the coding sequence for a reverse transcriptase-like enzyme in a transposable genetic element in *Drosophila melanogaster.* Nature. 312: 659–661.

Schnable et al., 2009. The B73 maize genome: complexity, diversity, and dynamics. Science. 326:1112–1115.

Singer-Sam J, Riggs A, In J, Saluz H, 1993. DNA Methylation: Molecular Biology and Biological Significance. BirkhauserVerlag, Boston, MA. 358–384.

Siomi C, Sato K, Pezic D, Aravin A, 2011. PIWI-interacting small RNAs: the vanguard of genome defence. Nat. Rev. Mol. Cell. Biol. 12: 246-258.

Slotkin K, Martienssen R, 2007. Transposable elements and the epigenetic regulation of the genome. Nat. Rev. Genet. 8:272–285.

Song U, Gerasimova T, Kurkulos M, Boeke J, Corces V, 1994. Anenv-like protein encoded by a *Drosophila* retroelement: evidence that gypsy is an infectious retrovirus. Genes Dev. 8: 2046–2057.

Strahl D, Allis D, 2000. The Language of Covalent Histone Modifications. Nature. 403: 41-45.

Teixeira K, Heredia F, Sarazin A, Roudier F, Boccara M, Ciaudo C, Cruaud C, Poulain J, Berdasco M, Fraga MF, et al., 2009. A role for RNAi in the selective correction of DNA methylation defects. Science. 323:1600–1604.

Tolia H, Joshua-Tor L, 2007. Slicer and the argonautes. Nat. Chem. Boil., 3: 36-43.

Torres-Martínez S, Ruiz-Vázquez M, 2017. The RNAi Universe in Fungi: A Varied Landscape of Small RNAs and Biological Functions. *Annu. Rev. of Microbiol.* **71**, 371–391, https://doi.org/10.1146/annurev-micro-090816-093352

Tosa Y, Nakayashiki H, Hyodo H, Mayama S, Kato H, Leong SA. 1995. Distribution of retrotransposon MAGGY in *Pyricularia* species. Ann. Phytopathol. Soc. Jpn. 61:549–554.

Murata T, Kadotani N, Yamaguchi M, Tosa Y, Mayama S, H. 2007. siRNA-dependent and -independent post-transcriptional cosuppression of the LTR-retrotransposon MAGGY in the phytopathogenic fungus *Magnaportheoryzae. Nucleic Acid Res.* 35(18): 5987–5994.

Tristem M, Kabat P, Herniou E, Karpas A, Hill F, 1995. Easel, a gypsy LTR-retrotransposon in the *Salmonidae*. Mol. Gen. Genet. 249: 229–236.

Tucker L, 2001. Methylated cytosine and the brain: a new base for neuroscience. Neuron. 30: 649–652.

Ulrike S, Olivia D Laura L, Walter H, Dixie M, Brian S, Christine L, 2009. Human Endogenous Retroviral Long Terminal Repeat Sequences as Cell Type-Specific Promoters in Retroviral Vectors. Journal of Virology. 12643-12650.

Urashima S, Hashimoto Y, Don D, Kusaba M, Tosa Y, Nakayashiki H, and Mayama S, 1999. Molecular analysis of the wheat blast population in Brazil with a homolog of retrotransposon MGR583. Annu. Phytopathol. Soc. Jpn. 65, 429-436

Vasquero A, Loyola A, Reinberg D, 2003. The Constantly Changing Face of Chromatin. Science of Aging Knowledge Environment. 14:RE4.

Voytas F, Ausubel F. 1988.A *copia*-like transposable element family in *Arabidopsis thaliana.* Nature. 336: 242–244.

Vu B, Pham K, Nakayashiki H, 2013. Substrate-induced transcriptional activation of the MoCel7C cellulase gene is associated with methylation of histone H3 at lysine 4 in the rice blast fungus *Magnaporthe oryzae*. Appl Environ Microbiol. 79: 6823-6832.

Wagner R, Busche S, Ge B, Kwan T, Pastinen T, Blanchette M, 2014. The relationship between DNA methylation, genetic and expression inter-individual variation in untransformed human fibroblasts. Genome Biology. 15(2):R37.

Wang H, Zhang X, Liu J, Kiba T, Woo J, Ojo T, Hafner M, Tuschl T, Chua H, Wang J, 2011. Deep sequencing of small RNAs specifically

associated with Arabidopsis AGO1 and AGO4 uncovers new AGO functions. Plant J. 67(2):292-304.

Wang Q, An B, Hou X, Guo Y, Luo H. He C, 2018. Dicer-like proteins regulate the growth, conidiation, and pathogenicity of Colletotrichum gloeosporioides from Hevea brasiliensis. Front. Microbiol. 8:2621. doi: 10.3389/fmicb.2017.02621.

Wei H, Zhou B, Zhang F, Tu Y, Hu Y, Zhang B, Zhai Q, 2013. Profiling and identification of small rDNA-derived RNAs and their potential biological functions. PLoS One. 8: e56842.

Weiberg A, *et al*., 2013. Fungal Small RNAs Suppress Plant Immunity by Hijacking Host RNA Interference Pathways. *Science (New York, N.Y.)* **342**, 118–123, https://doi.org/10.1126/science.1239705

Wicker T, Sabot F, Hua-Van A, Bennetzen JL, Capy P, Chalhoub B, Flavell A, Leroy P, Morgante M, Panaud O, et al., 2007. A unified classification system for eukaryotic transposable elements. Nat Rev Genet. 8:973–982.

Wu J, Yang Z, Wang Y, Zheng L, Ye R, Ji Y, Zhao S, Ji S, Liu R, Xu L, et al., 2015. Viral-inducible Argonaute18 confers broad-spectrum virus resistance in rice by sequestering a host microRNA. eLife. 4.

Yoder J, Walsh C, Bestor T, 1997. Cytosine methylation and the ecology of intragenomic parasites. Trends Genet.13:335–340.

Youngson RM, 2006. Collins Dictionary of Human Biology. Glasgow: HarperCollins.

Zentner E, Henikoff S, 2013. Regulation of Nucleosome Dynamics by Histone Modifications. Nature Structural & Molecular Biology, 20, 259-266. http://dx.doi.org/10.1038/nsmb.2470

Zhang X, Shiu S, Cal A, Borevitz JO, 2008. Global analysis of genetic, epigenetic and transcriptional polymorphisms in *Arabidopsis thaliana* using whole genome tiling arrays. PLoS Genet. 4

Zhang X, 2008. The epigenetic landscape of plants. Science. 320:489–492.

Zhu H, Hu F, Wang R, Zhou X, Sze H, Liou W, Barefoot A, Dickman M, Zhang X, 2011. *Arabidopsis* Argonaute10 specifically sequesters miR166/165 to regulate shoot apical meristem development. Cell 145: 242-256.

Zilberman D, Gehring M, Tran RK, Ballinger T, Henikoff S, 2007. Genome-wide analysis of Arabidopsis thaliana DNA methylation uncovers an interdependence between methylation and transcription. Nat Genet. 39:61–69.